Politecnico di Torino

Politecnico di Torino

Master's Degree in Mechanical Engineering

Academic Year 2024/2025

Optimization of build orientation in additive manufacturing: a comparative evaluation of algorithms and critical review

Supervisor:

Prof. Flaviana Calignano

Co-Supervisor:

Prof. Schleifenbaum Johannes Henrich

Ing. Pletzer-Zelgert Leonie Pauline

Student:

Mattia Santini

Abstract

The study investigates the optimization of build orientation in additive manufacturing, an influential factor affecting mechanical properties, surface and part quality, and process efficiency. Two orientation evaluation strategies are compared: the commercial software Autodesk Netfabb and a novel multi-criteria algorithm developed at RWTH Aachen University.

The proposed algorithm is designed to minimize thermally induced deformation during printing with Powder Bed Fusion – Laser Beam Melting technology. It employs six Key Performance Indicators (KPIs) derived from part geometry, which are evaluated on a layer-by-layer basis to assess deformation risk. While the study identifies correlations between geometric KPIs, the orientation ratings generated by the algorithm exhibit inconsistencies and limited reliability. The method is benchmarked against Autodesk Netfabb's commercial orientation tool, which utilizes a multi-objective optimization approach, using a shared dataset of test parts.

The critical comparison highlights the respective strengths and limitations of both approaches and proposes directions for future methodological improvements in defining build orientation.

Keywords: Additive Manufacturing, Build Orientation, Thermal Deformation, Optimization Algorithm

Table of Contents

List of abbreviations

KPI	Key indicator of performance
AM	Additive manufacturing
FDM	Fused deposition modelling
SLA	Stereolithography
DfAM	Design for additive manufacturing
MJF	Multi jet fusion
SLS	Selective laser sintering
PBF-LB/M	Laser Beam Powder Bed Fusion – Metals
DED	Directed Energy Deposition
PBF-EB/M	Electron Beam Powder Bed Fusion – Metals

List of figures

List of tables

1 Introduction

Additive manufacturing (AM) is a group of technologies which are defined by the normative ISO/ASTM 52900 as: “A process of joining materials to make parts from 3D model data, usually layer upon layer, as opposed to subtractive and formative manufacturing methodologies”. These AM technologies developed themselves with multiply group of materials, the most relevant in terms of applications and distribution are polymers and metals. Additive manufacturing is most widely utilized in the aerospace, automotive and medical industries (Vafadar et al. 2021).

The study focuses on the definition of print orientation in additive manufacturing and its role in the decision-making process, emphasizing the impact of orientation on the quality and performance of the final components. To explore this issue, a comparative analysis was carried out between orientation strategies produced by widely used commercial software and those generated by a novel optimization algorithm developed at RWTH Aachen University. The in-house algorithm adopts a multi-objective approach, integrating geometric criteria to identify orientations that balance competing requirements. The comparison aimed to assess the effectiveness and limitations of both approaches in achieving optimal build orientations.

1.1 Influence of the orientation

Despite the development that AM technologies have undergone since their invention; they still suffer from problems relating to the reproducibility and repeatability of the process. These obstacles related to the repeatability has an influence also on quality of the components printed with additive technologies. One of the most important parameters for the determination of the quality of the component is the build orientation. Indeed, the build orientation play a significant role in many aspects of the results of the components for both class of materials: polymeric and metals. Build orientation is the spatial arrangement of a 3D model within the build chamber of an additive manufacturing system, characterized by its rotation angles about the X, Y, and Z axes of the building plate. It determines the sequence and direction of layer deposition.

There are some differences in the effects of the orientation on the different materials and technologies.

1.1.1 Polymeric

The build orientation during the printing of components in plastic material has an impact on different areas:

- Support structures: in many of the plastic AM technologies the use of support is necessary, indeed they are used in fused deposition modelling (FDM, tradename of Stratasys) and Stereolithography (SLA). These structures are necessary to avoid collapses of the component during its construction and in some cases as in also of protections.

  Support structures are also related or responsible for several negative effects. The massive presence of supports leads to an increase in overall costs. Indeed, the amount of material needed to print the component increases, as does the time needed. In addition, post-treatment is needed to remove the support structures. These treatments can have little impact, as in the case of FDM with polymers that dissolve in water or specific solutions. But often, as in the case of technologies such as SLA and FDM with technical polymers, removal is more complex because the supports are in the same material as the component. Therefore, removal is often manual and there is a risk of damaging the component.
- Delamination: This phenomenon is the separation of two consecutive layers, this is due to poor adhesion between the layers and can also occur during printing leading to the failure of the construction. Delamination occurs mainly with composite materials because the introduction of fibers increases the anisotropy and the bonding between the matrix and the fibers is critical and related with the interfacial failure. Consequently, composite materials exhibit a significantly higher sensitivity to build orientation compared to the polymeric counterparts. Specifically, components fabricated in a horizontal orientation (parallel to the XY-plane) tend to demonstrate enhanced mechanical performance and reduced susceptibility to interlayer delamination.
- Mechanical properties: Numerous studies have investigated the influence of build orientation on various mechanical properties across different additive manufacturing technologies. Li studied the impact of the build orientation on the stereolithography with experiments based on destructive tests. He discovered that the tensile strength is highly influenced by printing orientation, however, elastic modulus is not affected significantly by the orientation. The study shows that

fracture toughness depends on the printing orientation, following a trend where toughness increases initially with orientation angle and then decreases, with a maximum at an intermediate angle. (Li e Teng 2024). Sedighi investigated the effect on the parts printed with FDM of the build orientation. The results are similar, indeed the elastic modulus did not undergo significant changes, while, fracture toughness and flexural strength showed a relevant correlation (Sedighi et al. 2020). Calignano examined the two polymeric powder bed fusion techniques: MJF (multi jet fusion) and SLS (selective laser sintering) with the same material: polyamide 12 (PA12). The results show a correlation between the mechanical properties and the build orientation for both technologies. Indeed, an anisotropy behaviour characterized both: SLS and MJF, however, SLS parts showed a greater sensitivity to orientation effects, which are particularly evident for the vertical sample. Parts made with MJF exhibited higher ultimate strength but lower toughness. Those evidence are explained with the different density, form and dimension of pores in the samples (Calignano et al. 2021)

- Surface roughness and surface quality: Due to the AM characteristic, surface roughness is influenced by the stair-stepping effect. This phenomenon depends on the height of the layer, in fact, as far as polymeric AM technologies are concerned, the most involved is FDM due to thicker layers. Chand suggested that the parts for the MJP-based 3D printing should be placed along the maximum area in contact with the base plate. It will provide better heat dissipation from the hot layers to the base plate, Result in more uniform cooling and material contraction and consequently in a better surface quality (Chand et al. 2023). The effect of the orientation on geometrical accuracy and surface roughness in parts printed with FDM is studied by Turek. The investigation determined that the orientation does not impact significantly the geometrical accuracy. In contrast the surface roughness is dependent to the build orientation. It is demonstrated that the horizontal surfaces has the lowest roughness, the angled surface that suffer the stair-stepping effect showed the highest roughness with intermediate results for the supported surfaces (Turek et al. 2024)
- Cost: the build orientation significantly affects the final cost of an additively manufactured component, primarily through two dependent parameters: the number of layers required, and the amount of waste material generated. The machine operating cost is closely related to the build time, determined by the number of layers, and to the volume of support structures, which in turn influences material

consumption. Raut, through his studies, confirms the relevance of these cost-driving factors specifically in the context of FDM (Raut et al. 2014).

1.1.2 Metal

As regards the production of metal components through additive manufacturing, there are problems with the plastic sector such as:

- Support structure: support structures are also essential in metal additive manufacturing and are present in all three of the most commonly used technologies: Laser Beam Powder Bed Fusion – Metals (PBF-LB/M), Directed Energy Deposition (DED), and Electron Beam Powder Bed Fusion – Metals (PBF-EB/M). In both PBF-LB/M and DED, these structures primarily serve a mechanical support function, with a secondary role in managing heat during the manufacturing process. Instead, in the case of PBF-EB/M the piece is supported by the powder itself, and the function of the supports is linked to thermal management. in this case the negative effects of using these structures are even more serious. the impact on costs is generally higher due to the higher cost per gram for metal powders. Furthermore, their removal is more complex and requires post-treatments.
- Mechanical properties: due to the nature of the process, components exhibit different mechanical properties in the XY plane compared to the Z direction, which is congruent with the building direction. This is particularly evident in some metals (Palmeri et al. 2022). This phenomenon is more pronounced for certain materials, furthermore the DED process is characterised by a lower adhesion between the layers, this leads to marked anisotropy. Part orientation allows the optimization of these properties based on expected loads. Moreover, the variability in microstructure related to the local thermal history affects mechanical properties, such as fracture behaviour, hardness and residual stresses (Mertens et al. 2020).
- Cost and time: the build orientation significantly influences the required printing time. Specifically, the number of layers, one of the main factors determining production time, is directly related to the height along the Z-axis, which is, in turn, dictated by the component's orientation. Furthermore, as previously discussed, orientation affects the need for support structures, which also contribute to increased printing time.

The cost of the component depends largely on the production time, as it is linked to machine usage duration and material waste. The latter is influenced by both the quantity and positioning of the support structures.

- Surface roughness: surface roughness is influenced by several factors, including layer height, laser parameters and part orientation. Roughness is higher on downskin surfaces due to phenomena related to the different thermal conductivity of the powder, such as balling or partially bonded particles. The balling effect increases the formation of discontinuous borders that occurs during the laser melting of the metal powder. Balling is the breakup of the molten pool into small entities. During the melting of metal powders, the high thermal gradient between different volumes of the molten material generates a difference in surface tension within the pool, which produces Marangoni convection. The partially bonded particles are observed at step edges due to insufficient heat during laser melting, preventing full sintering. As the sloping angle increases, the concentration of these particles rises because the step edges become more closely spaced (Strano et al. 2013)
- Thermal stresses and deformations: the processes of metal AM are susceptible to residual stresses and thermal distortions, which can compromise mechanical performance, dimensional accuracy, and overall part functionality. These issues are primarily caused by steep thermal gradients and rapid cooling rates resulting from the localized heating of the moving laser. This phenomenon, known as the thermal gradient mechanism, induces repeated expansion and contraction cycles that generate uneven thermal stresses, and, when exceeding the material's yield strength, plastic deformation and warping.

1.2 Algorithm of orientation

In AM, the orientation of a part within the build envelope is a pivotal parameter that significantly influences the overall quality, structural performance, and economic efficiency of the fabrication process. The determination of optimal part orientation constitutes a fundamental decision-making challenge in both polymer-based and metal-based AM technologies.

The complexity of this problem arises from the inherently multi-objective and often conflicting nature of the criteria involved. For instance, an orientation that minimizes support material may concurrently lead to suboptimal surface finish or increased residual

stresses, particularly in metal AM processes where thermal gradients play a dominant role. Conversely, in polymer AM, considerations such as anisotropic mechanical properties and surface quality become more pronounced.

To address these challenges, a range of algorithmic approaches has been developed, deterministic methods, heuristic optimization, evolutionary algorithms. These algorithms aim to systematically evaluate the trade-offs among competing objectives to arrive at a build orientation that best satisfies the functional and manufacturing requirements of the part.

1.2.1 Polymer

In the existing literature, a wide range of optimization algorithms has been developed, each tailored to specific additive manufacturing technologies and varying levels of geometric complexity. Among these, single-objective approaches, such as the algorithm proposed by Zwier which aim to minimize the use of support structures by identifying and analysing relevant geometric features (Zwier e Wits 2016) or the one developed by Zhang which minimize the build time and the cost of parts printed with SLS or SLA (Zhang et al. 2017). In addition, advanced algorithms based on multi-objective optimization have also been developed, aiming to simultaneously address multiple performance criteria thereby offering a more comprehensive approach to process optimization in additive manufacturing:

Matos proposes an optimization algorithm specifically tested on parts produced via FDM. The primary objective of the algorithm is to enhance process efficiency by minimizing the need for post-processing operations. To achieve this, the approach prioritizes multiple performance criteria, including geometric accuracy, surface finish, build time, and the volume of support structures required during fabrication. The optimization process integrates several evaluative metrics: volumetric error, surface quality and roughness, support-affected surface area, the stair-stepping effect, and the overall build height of the component, each of the parameters are geometric-based. These criteria collectively influence the quality and manufacturability of the final part. The optimization itself is performed using the Electromagnetism-like algorithm. (Matos et al. 2020)

Ransikarbum suggests an orientation algorithm for FDM and SLS based on multicriteria decision making, the parameters it takes into consideration are: Part cost, time, surface quality, part accuracy, support volume, mechanical property. The method is divided into three phases. First, the alternatives (e.g., different print orientations) and

the evaluation criteria are selected, recognizing that different decision makers may have different preferences and that DEA measures the relative efficiency without considering these preferences. In the second phase, DEA divides the alternatives into efficient and inefficient, while AHP is used to assign weights to the criteria based on the experience of the decision makers, but without directly ranking the alternatives. Finally, in the third phase, the data is normalized via Linear Normalization to combine the objective results of DEA with the subjective preferences of AHP, thus obtaining a final ranking that reflects both measurable data and expert judgments. (Ransikarbum et al. 2021).

A multi-attribute decision making is proposed by Qin. This method firstly quantifies the attributes of all alternative build orientations and then generates the optimal build orientations from the alternative. In the process are considered these parameters: surface roughness, part accuracy related with effects of shrinkage and distortion, volume of support structure, mechanical strength mainly connected to the anisotropy, build time and cost and post-processing for the surface quality or mechanical properties in particular area (Qin et al. 2019)

1.2.2 Metal

In the scientific literature, a wide variety of build orientation optimization algorithms has been developed, tailored to different additive manufacturing technologies, most notably powder bed fusion and directed energy deposition, each of which presents distinct challenges and process constraints. These algorithms are designed to determine optimal part orientations that simultaneously minimize support material usage, reduce build time, enhance thermal management, and improve mechanical integrity.

Typically, such optimization strategies adopt multi-objective frameworks, integrating geometric evaluations (e.g., overhang and surface accessibility analysis), physics-based simulations (e.g., thermal gradients, residual stress predictions), and manufacturability constraints specific to the AM process in use. Advanced methodologies employ heuristic optimization techniques such as genetic algorithms, simulated annealing, or swarm intelligence, as well as machine learning models and rule-based decision systems. These tools allow for the systematic exploration of a high-dimensional design space, often evaluating thousands of candidate orientations to identify configurations that represent optimal trade-offs among functional performance, structural reliability, and production efficiency.

By providing data-driven guidance for orientation selection, these algorithms significantly contribute to the development of more robust, cost-effective, and reliable metal additive manufacturing workflows.

Williems introduces an orientation optimization algorithm developed for the PBF-LB/M. The method is based on eight cost functions based on the following parameters: supports, contact possibility with recorders, roughness, cost, deformations (calculated with FEM simulations), part height, area in contact with the print bed. The computation of deformations via simulations is limiting and only a subset of all orientations is tested. (One of the main challenges addressed is the computational cost of distortion analysis. To address this issue, the paper proposes a response surface method that uses finite element analysis on a sample of orientations to approximate distortion along the orientation space.) These cost functions are then normalized and combined using a user-defined weighted sum to reflect different manufacturing priorities.

A Monte Carlo optimization algorithm is used to explore an orientation space discretized into three angular degrees of freedom. The flexibility in weight assignment makes the formalism adaptable to specific component geometries and industrial use cases (Willems e Megahed 2022).

Mele proposes an optimization algorithm that uses an overall fitness function based on multiple factors: build time, support volume, deformation and surface roughness (Mele et al. 2022). This approach provides flexibility by allowing different weights to be assigned to each factor. However, the calculation of deformation is simplified, as it only considers the presence and geometry of overhanging structures. the minimization of the overall fitness function is obtained with a genetic algorithm.

Baccagli introduces an algorithm specifically designed for industrial-scale additive manufacturing, aimed at optimizing the orientation of components to significantly reduce support volume and minimize processing times. Their approach uniquely applies selective ray tracing only to surface triangles that form overhangs and therefore may require support structures. Integration with an improved Particle Swarm Optimization algorithm enables rapid exploration of the orientation space to find the optimal orientation through iteration, reducing the processing times of other algorithms (Bacciaglia et al. 2024).

Gonzalez proposes a method for determining the optimal orientation of parts in PBF-LB/M based on a temperature-driven indicator. This method aims to reduce thermal

gradients during the manufacturing process, which benefits microstructural integrity, minimizes deformations, and lowers residual stresses. The proposed index takes into account several factors, including the ability to dissipate heat through the build plate, the cross-sectional area which influences heat accumulation, the height of the build since taller parts tend to increase heat accumulation, and the angle of the surfaces that also affect thermal gradients. The index is calculated for each possible orientation, and the orientation that minimizes this parameter is selected as the most suitable for printing. (González et al. 2025)

1.2.3 Commercial software

In the industrial landscape of Additive Manufacturing, numerous commercial software solutions have been developed to ensure efficiency, high quality, and process reliability. These tools are designed to manage not only the decision-making phase related to part orientation but also the entire sequence of operations from the STL file to the final build preparation, while meeting stringent time constraints. Most of these systems are based on multi-objective optimization algorithms, enabling the evaluation and balancing of competing criteria such as support volume, build time, and surface quality.

The market offers a wide range of solutions, including software developed by AM machine manufacturers, such as EOSPRINT and 3DXpert, or more versatile platforms that are compatible with various printing systems and materials. These are capable of optimizing orientation for both polymer and metal components. In this context, particular attention will be devoted to Autodesk Netfabb and Materialise Magics

Materialise Magics: materialize magics orientation optimization algorithm is based on 5 parameters, these are:

I. Z-height (build height)
II. Support surface
III. Maximal cross section
IV. XY projection
V. Support on marked

Depending on the specific AM technique employed, various parameters influence the optimal orientation of a part. A key factor common to all AM processes is the build height (Z-height), which directly impacts the total build time. Minimizing the Z-height generally leads to shorter fabrication times and, in certain processes, contributes to

reduced material consumption, especially in technologies involving expensive feedstocks.

For instance, In SLA, two orientation-related criteria are particularly significant: the minimization of support surface area and the minimization of XY projection area. Reducing the surface area that requires support not only saves material but also decreases post-processing time, leading to more efficient production. On the other hand, minimizing the XY projection area allows for denser packing of multiple parts on a single build platform, thereby improving throughput. However, these criteria often conflict with the goal of minimizing build height, necessitating trade-off decisions during orientation optimization.

In Laser Sintering, particularly in metal AM, the formation of large cross-sectional areas is generally discouraged. Such geometries tend to accumulate significant thermal stresses during layer-by-layer construction, which can result in part deformation or failure. Orientation strategies in these processes must therefore aim to distribute thermal loads more evenly and avoid configurations that exacerbate stress concentration.

Additionally, in many AM techniques, support structures are essential for the successful fabrication of overhanging or inclined features. However, there are often critical surfaces where support structures are undesirable, typically due to difficulties in post-processing or surface quality requirements. The criterion known as “Support on marked” quantifies the percentage of a user-defined area that would require support. Lower values are preferred, as they imply less interference with critical part features and reduced post-processing complexity.

Autodesk Netfabb: Netfabb algorithm after the definition of the workspace and other information such as the critical angle, is based on a multi-objective optimization. the optimization parameters are:

I. supported area
II. support volume
III. bounding box volume
IV. part height
V. center-of-gravity height
VI. unsupported triangles

Netfabb by default uses these 6 parameters to perform a classification of the different orientations tested. then by assigning the same value to each of the items it draws up

an overall classification to determine the best orientation. it is possible to go and modify the weight assigned to each of the parameters to accommodate the differences and needs of the different technologies and the different components to be printed.

The first two parameters (*supported area, support volume*) are related to the minimization of the support structures, with the consequent reduction of waste material, cost and necessary post-processing. The parameter *bounding box volume* is related with the optimization of the volume of chamber occupied for the single component in a multi-parts job. The parameter *part height* has an impact on the building time and could influence also the amount of support structures needed. The reduction of the *center-of-gravity* height parameter leads to a more stable process in the case of stresses during the printing phase such as the movement of the recoater. Furthermore, in particular for metal powder bed technologies, the heat dispersion towards the base is improved, Finally, the presence of *unsupported triangles* is primarily associated with the increased need for support structures and, consequently, with the extent of post-processing required.

Both software tools are not specific for a single technology and do not differentiate between polymer- and metal-based additive manufacturing processes. However, such distinctions can be introduced by appropriately adjusting the weights assigned to each evaluation parameter.

1.3 Design for Additive Manufacturing

The advent of additive manufacturing has required the formulation of component design rules; this is because the nature of the process based on the successive deposition of layers is at the antithesis of pre-existing traditional industrial technologies. Consequently, the rules that had been developed and tested for traditional technologies are not able to provide any guarantee of quality and efficiency for parts printed in additive manufacturing. Furthermore, they do not allow to exploit the potential that additive is able to provide such as light structures, variable mechanical properties, complex geometries and it highlights its limits such as construction times. The rewriting of the design rules for this technology is called Design for additive manufacturing (DfAM).

DfAM signifies a fundamental shift in the way products are conceptualized, designed, and fabricated. By applying the advantages of additive manufacturing, DfAM enables the creation of geometries and structures that are difficult or even impossible to achieve with traditional manufacturing techniques. While AM offers unprecedented design

freedom and the ability to fabricate complex parts, it also introduces specific process-related constraints. Addressing these limitations requires tailored design strategies, collectively referred to as DfAM, that ensure manufacturability, structural integrity, and functional performance within the context of additive technologies (Asapu e Ravi Kumar 2025a). DfAM is created by a set of principles, workflows, rules and design methods specifically adapted to the characteristics of additive processes. It aims to improve the functionality, manufacturability, customization and performance of components by integrating material behaviour, process constraints and geometric freedom early in the product development cycle. However, these methodologies are not yet totally unified and there are discrepancies between the sets of rules and workflows.

The first step of DfAM is the definition of the functionality required for the piece. In this phase, the constraints on the geometry to be respected, the mechanical performance required for the component and consequently also the conditions of existence of the component in terms of load, temperature and aggressive environments (example: conditions of high corrosion) are defined.

The next step involves defining the additive manufacturing technology to be used, along with selecting the appropriate material. These two decisions must be made concurrently, as the compatibility between material and process is critical. Certain materials can only be processed using specific AM technologies. Moreover, each technology imposes distinct design constraints, including differences in printing speed, the necessity and type of support structures, achievable surface quality, and the minimum feature size that can be reliably produced. These factors must be carefully considered to ensure the feasibility and quality of the final part.

The next phase includes the definition of the specific geometry, the choice of process parameters and orientation and the simulation of the component and the process.

In the geometry definition phase, the rules of traditional technologies are no longer used, but we try to fully exploit the potential of AM specifically in terms of freedom and complexity that it can ensure without a relevant increase of the production cost. despite the freedom some articles still provide rules to respect DfAM: Application of the design rules in the early design stages (rules regarding the minimum dimensions of some features such as holes, walls. or the maximum dimensions of other features to be self-supporting: channels and bridges, angles to be respected to avoid having to use support structures) (Djokikj e Kandikjan 2023).

In this phase, advanced design methodologies such as topology optimization and lattice structures are employed primarily to achieve weight reduction and to model the mechanical behaviour of the component. Additionally, generative design techniques are utilized to explore multiple design alternatives, based on the boundary conditions and loading scenarios defined in earlier stages of the process. This exploration is enabled through the application of evolutionary algorithms, which iteratively converge toward optimal geometries. These combined strategies not only allow for significant mass reduction but also enhance structural performance by leveraging the design freedoms afforded by additive manufacturing.

As previously emphasized, the selection of build orientation represents a critical step in ensuring both the quality and performance of additively manufactured components, as it influences multiple factors. Consequently, this decision is frequently supported by computational algorithms and multi-objective optimization frameworks aimed at balancing these competing criteria or through the experience and know-how of the designers. The placement of this step within the overall design and manufacturing workflow is not fixed. In most cases, it is carried out after the geometric design of the part has been finalized, as observed in the algorithms discussed previously. However, several alternative approaches exist, which integrate orientation selection at earlier stages or in parallel with other optimization processes. The following are some representative alternatives: It is proposed the early determination of the part orientation (Leutenecker-Twelsiek et al. 2016). This methodology defines the build orientation prior to the final design stage, in contrast to conventional approaches where orientation is typically selected afterward. Here, orientation is determined immediately after the conceptual design phase and is based on the analysis of geometric features that are prioritized according to parameters such as surface quality, dimensional accuracy, part distortion, support structure requirements, and build height. This approach is motivated by findings reported in Adam's study, which indicate that a significant portion DfAM guidelines, approximately 70% for SLM and FDM processes, are directly influenced by the chosen build orientation (Adam e Zimmer 2014).

An alternative approach, distinct from the previously discussed strategies, involves a deeper integration of the design phase with the orientation decision-making process. As illustrated in Figure 1.1, this methodology proposes the implementation of an iterative workflow that includes the design and geometry modification stage, the printability assessment phase, and the build orientation selection. This integrated process

enables the optimization of part geometry not only to increase functional performance but also to improve manufacturability. In particular, by iteratively modifying the geometry with consideration of print constraints, it becomes possible to reduce the reliance on support structures and facilitate a more efficient and reliable additive manufacturing process (Asapu e Ravi Kumar 2025b).

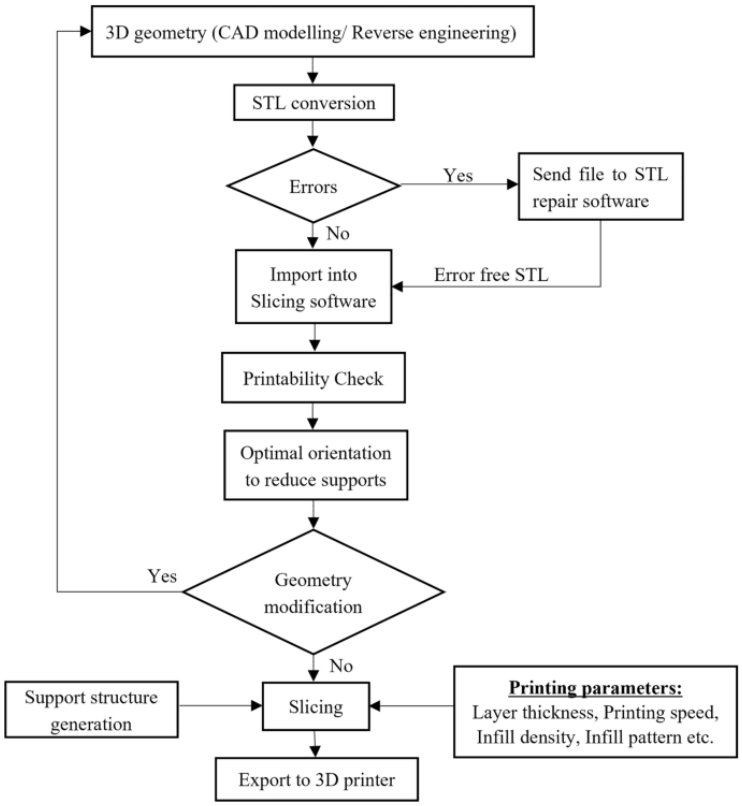

Figure 1.1: workflow with iterative cycle of geometry modification and orientation choice

In the concluding stage, Finite Element Analysis and process simulations are employed to evaluate the mechanical performance of the part under realistic operating conditions and to anticipate potential manufacturing challenges, such as warping, delamination, or overhang collapse.

Finally, the DfAM workflow includes accounting for post-processing requirements, including surface finishing, heat treatment, and machining allowances.

2 RWTH algorithm

In this chapter the model developed at RWTH Aachen University is presented. The objective of the research is to develop and validate an algorithm capable of ranking various build orientation, specifically for PBF-LB/M, based on the minimization of thermal distortion in the printed component, without the need for computationally intensive thermal simulations. The study focuses exclusively on the effect of the component's geometry on thermal behaviour and the resulting deformation, deliberately excluding other potential variables such as laser parameters, that could influence the outcome. For consistency, the same material was used in all the simulations and for all the parts considered in the study. The idea is to compare the FEM thermal simulation results with KPIs to develop an algorithm capable of ranking the various orientations based on the influence of geometry on thermal deformation.

2.1 Source of deformation

The PBF-LB/M process is susceptible to relevant residual stresses and thermal deformations. In the worst cases even warping, these kinds of defects can compromise mechanical performance, part accuracy and functionality (B. K et al. 2021). The comprehension and the control of the phenomenon and amplification factors is a critical point to increase the quality of the component.

Thermal distortion in PBF-LB/M is mainly related to thermal gradients, on the order of hundreds of degrees Celsius per second and cooling rates created by the localized heating generated by the moving laser (Tabaie et al. 2020). During the scanning process, multiple thermal cycles occur, during which the temperature in the laser spot area reaches at least the material's melting point. The surrounding material experiences expansion due to the elevated temperature. This expansion is subsequently followed by contraction as the temperature rapidly decreases. This process is called thermal gradient mechanism; it leads to uneven thermal stresses and where the those exceed the yield strength also plastic deformation (Song et al. 2020) . Many studies show that the thermal gradient mechanism and its effects can be attenuated with the optimization of the build parameters: laser power, scanning and hatching strategy (Tucho et al. 2018; Manikandan e Venkatesan 2024; Yi et al. 2019), the geometrical features and parameters related with the geometry (Mercelis e Kruth 2006; Buchbinder et al. 2013; Oliveira et al. 2020). Focused on the last two points:

- Downskin surface: this type of feature is related to problems of deformation due to the arrangement of the powder, which is characterized by significantly lower thermal conductivity compared with the melted material as revealed by Ranjan (Ranjan et al. 2020). The powder leads to a poor heat dissipation in the area which causes phenomena of heat accumulation. The intensity of the phenomenon is related also to the angle of the downskin surface. In the study of Parry, it is shown that the presence of heat accumulation in the component leads to an intensification of the residual stresses in those areas, which can also lead to deformations (Parry et al. 2019). Additionally, Mele investigates the influence of the characteristics of the downskin surface (Mele et al. 2021). Deeply, the experimental study is focused on some characteristics: length, inclination angle, support density and thickness. The results show that main contribution for the displacement comes from the combination of inclination angle and thickness of those structures, while the interaction between support density and thickness has the main impact in the presence of warping. The contribution of the different factors could lead to both positive and negative displacement from the original geometry.
- Branches: this geometrical characteristic can cause residual stress and even deformations. Indeed, heating and cooling rates can vary significantly within the part for the presence of thermally independent areas. This leads to possible thermal gradients that cause stress and deformations to arise (Adam e Zimmer 2014).
- Transition of geometry: in this type of feature, you encounter heat accumulation and thermal gradients. These are caused by different cooling rates due to the different energy input and the different interactions with the powder, which cause different thermal dissipation. Thermal gradients within the molten material are responsible for deformations that are created (Adam e Zimmer 2014).

2.2 Parts

During the experiment, eight parts are being analysed; these are showed in the Figure 2.1. The parts were selected to represent a wide range of features that are characteristic of parts manufactured through AM. The selection aimed to examine various geometric characteristics to ensure that the study captures the typical challenges encountered in AM production. The features considered are transition thin to massive, sharp edges, pipes, thin walls and grids.

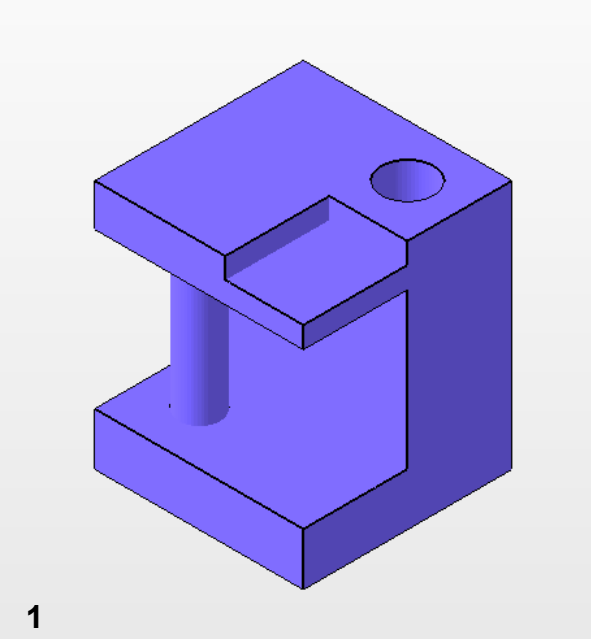

1

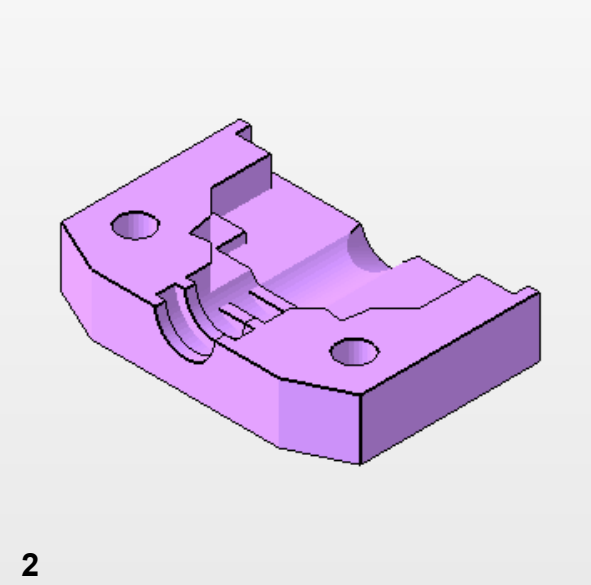

2

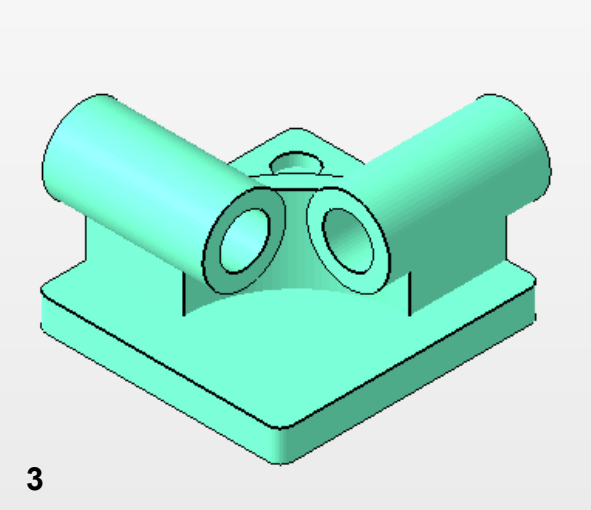

3

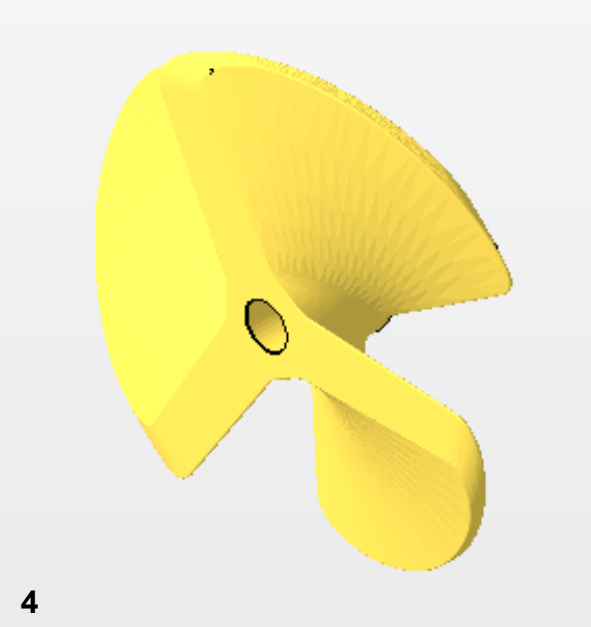

4

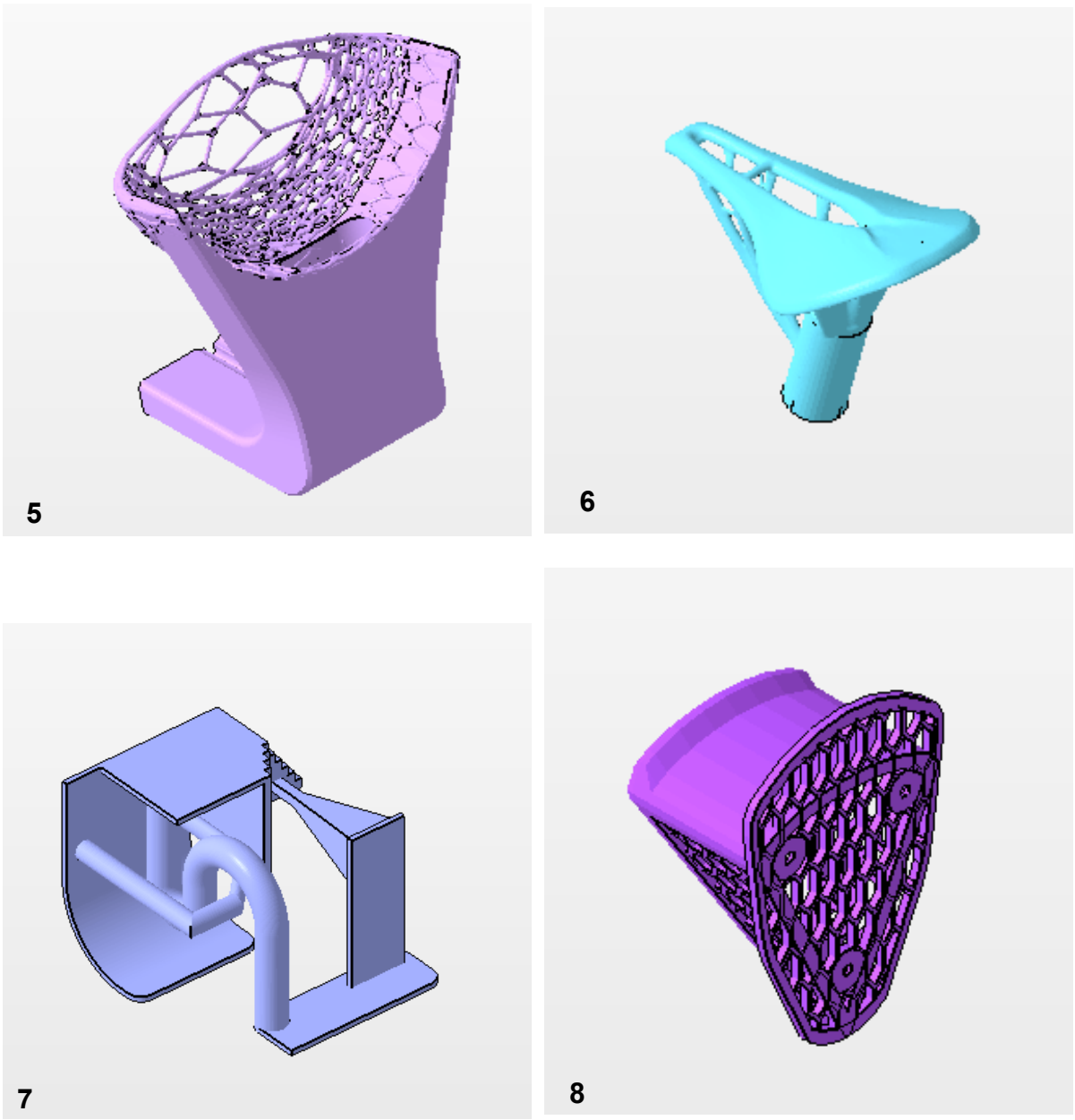

Figure 2.1: the 8 parts selected for the study, with the corresponding part-ID. Parts are order with an increasing volume to surface (deep-geometry; printables; thingiverse)

These different features were selected to examine their potential influence on the thermal history of the parts and how this thermal behaviour impacts the geometric accuracy quality of the final parts.

Additionally, the parts are evaluated using their surface-to-volume ratio, which provides a straightforward and effective method for quantifying the complexity of the geometry. A higher ratio often indicates more complex shapes.

To ensure comparability of data and control the computational effort required for thermal simulations, the dimensions of the parts have been standardized to the same value

for all the examined parts. Each part must be circumscribed in a cube with the side of 36 mm. This alignment allows for a more controlled analysis of how different features affect thermal behaviour, without introducing variability due to size differences.

2.3 Simulation

In the study, the simulations are conducted with Ansys Additive 2024. More specifically, it is used the *Thermal strain* simulation.

Each of the part is simulated in several orientations.

Part 1 is simulated in 30 orientations, with steps of 60° along the x-axis and steps of 36° along the y-axis. The possible rotation angles around the x-axis range from 0° to 360°, while for the y-axis, the angles range from 0° to 180° to avoid repeating the same orientations.

Parts from 2 to 8 are simulated in 18 orientations: with steps of 60° along the x-axis and steps of 60° along the y-axis. With the same considerations done for the Part 1.

2.3.1 Machine parameters and Material

The investigation focuses only on the influence of the component's geometry. Therefore, to ensure consistency, the thermal simulations were conducted using the same machine configuration, reported in Table 2.1. to delete the influence of the printed and other parameters like laser power, layer height and hatch distance. The same principle is used for the material. Steel 316L is selected for the thermal analysis and the calculation of the KPI. The properties of the material are declared in Table 2.2.

Table 2.1: machine parameters

Parameter	**Value**
Machine	Generic
Baseplate Temperature (°C)	80
Layer Thickness (µm)	50
Starting Layer Angle (°)	57
Layer Rotation Angle (°)	67
Hatch Spacing (µm)	100
Slicing Stripe Width (mm)	10
Laser Beam Diameter (µm)	100
Laser Power (W)	195
Scan Speed (mm/s)	1000

Table 2.2: characteristics of the material

Parameter	**Value**
Material	316L
Stress Mode	Linear Elastic
Elastic Modulus (GPa)	175
Poisson Ratio	0,27
Yield Strength (MPa)	494
Support Yield Strength Ratio	0,4375
Strain Scaling Factor	1
Anisotropic Strain Coefficients (||)	1,5
Anisotropic Strain Coefficients (⊥)	0,5
Anisotropic Strain Coefficients (Z)	1

2.3.2 Voxel dimension

An essential step for the correct realization of the research is the voxel dimension utilized for the thermal simulation with Ansys Additive 2024. The voxel dimension affects heavily the precision of results of the simulations and, on the other hand, also the computational cost and the time required to the obtain the results.

To guarantee a good trade-off between a restrained computational cost and reliable results, a comparative analysis has been made for each part for two random orientations between different voxel dimensions. The data from the thermal simulations were considered to make the comparative analysis average displacement for each layer. In each test conducted to determine the voxel dimension, the starting measurement was 0,5 mm, as suggested by (Mayer et al. 2020). Subsequently, other simulations are carried out with progressively smaller dimensions to obtain greater precision. When similar trends are observed between two voxel dimensions, the larger dimension is selected to minimize computational load. Trends are considered in the analysis as it focuses on ranking different orientations rather than relying on precise numerical values.

The results of the investigation of the voxel dimension are summarised in Table 2.3.

Table 2.3: overview of the voxel dimension for each part

Part-ID	**Voxel dimension [mm]**
1	0,5
2	0,5
3	0,5
4	0,25
5	0,25
6	0,25
7	0,25
8	0,25

2.4 KPIs

The calculation of the KPI is based on the geometry of the parts. The KPIs are calculate not only on the CAD model but also with information about the geometry extrapolated from the STL file. STL files could give more precise point of view of the component and can give a more complete analysis of the component, indeed, it also makes it possible to analyse the geometric characteristics of each individual layer.

The KPIs utilized to create the algorithm are:

- Massiveness: This describes the geometric position of the component volume in the building direction.

$$f_{massiveness} = \frac{1}{z_{Centroid} + 1} \tag{2.1}$$

$$z_{Centroid} = \frac{\sum_{i=1}^{N} V_i \times z_i}{\sum_{i=1}^{N} V_i} \tag{2.2}$$

  If the material is concentrated in the lower region, heat dissipation is facilitated through the base plate of the chamber, aiding in more effective heat management during the printing process.

- Contour-vector: Jumps of close contour block number between layers.

$$\Gamma_{i,cont-vec} = \{\gamma_{i,cont-vec} \,|\, \gamma_{i,cont-vec} = c_{i+1} - c_i \; with \; 0 < i \leq N\} \tag{2.3}$$

  It indicates geometrical changes and consequentially probable formation of deformation caused by thermal stress (Ranjan et al. 2020).

- Amounts of branches: it considered the number of thermally independent zones in each single layer.

$$\Gamma_{i,branches} = \{\gamma_{i,branches} \,|\, \gamma_{i,branches} = b_i \; with \; 0 < i \leq N\} \tag{2.4}$$

  The presence of multiple thermally independent zones results in distinct areas of energy input and heat dissipation, each exhibiting unique characteristics that lead to varying thermal behaviours across the different branches (Ranjan et al. 2020).

- Branches surface ratio: it quantifies the ratio between the largest and smallest surface areas of the branches within the layer.

$$\Gamma_{i,b-s\ ratio} = \left\{ \gamma_{i,b-s\ ratio} \,\middle|\, \gamma_{i,b-s\ ratio} = \left(\frac{\max\limits_{1<f<b}(a_f) - \min\limits_{1<f<b}(a_f)}{\max\limits_{1<f<b}(a_f)} \right)_n \ with\ 0 < i \leq N \right\} \quad (2.5)$$

Significant differences between branch surfaces increase the likelihood of different thermal behaviour in the independent areas, leading to an increase in deformation (Ranjan et al. 2020). As reported in Figure 2.2.

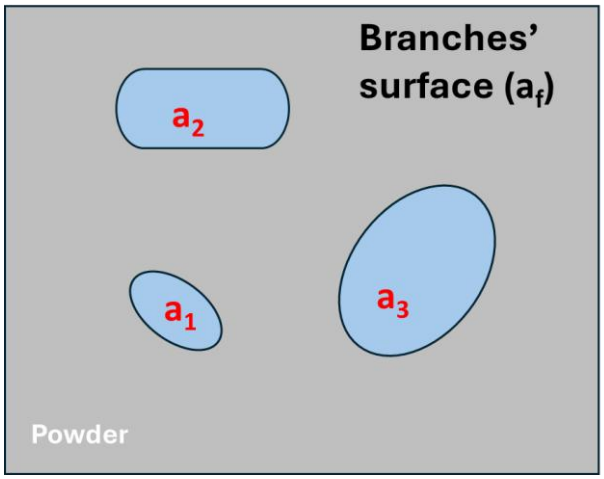

Figure 2.2: representation of the elements necessary for calculating the KPI**:** Branches surface ratio

- Downskin surface: this KPI investigates the influence of the variation of the surface between consecutive layers.

$$\Gamma_{i,ds} = \left\{ \gamma_{i,ds} \,\middle|\, \gamma_{i,ds} = \max_i \left(0, \frac{A_{i+1} - A_i}{A_{i+1}} \right) with\ 0 < i \leq N \right\} \quad (2.6)$$

This parameter is related to the different conductivity of the powder and the melted material, the powder as a conductivity around the 10% of the melted material (Alkahari et al. 2012). This parameter influences the heat dissipation and the possibility of arising of issue related with heat accumulation (Ranjan et al. 2020). As reported in Figure 2.3.

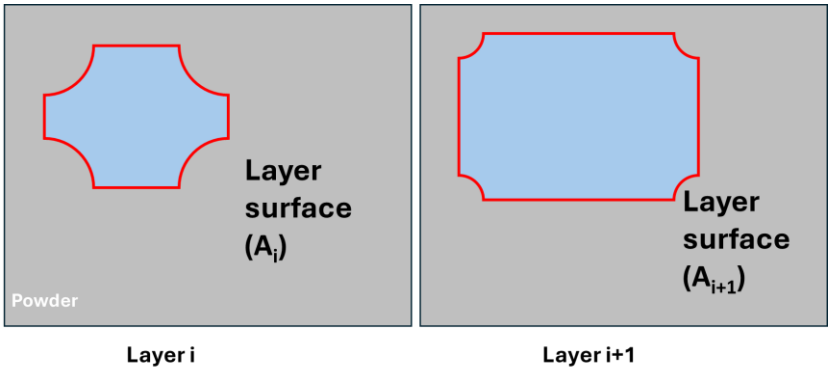

Figure 2.3: representation of the elements necessary for calculating the KPI**:** Downskin surface

- Powder to layer surface: the printed surface of each layer and the perimeter of this area are considered in this KPI.

$$\Gamma_{i,p-l} = \left\{ \gamma_{i,p-l} \,|\, \gamma_{i,p-l} = \left| \frac{A_i}{O_i} \right| \; with\; 0 < i \leq N \right\} \tag{2.7}$$

This KPI, like the previous one, takes into account the influence of the powder and its limited thermal conductivity. The focus here is on heat dissipation within the current layer. A representation is in Figure 2.4.

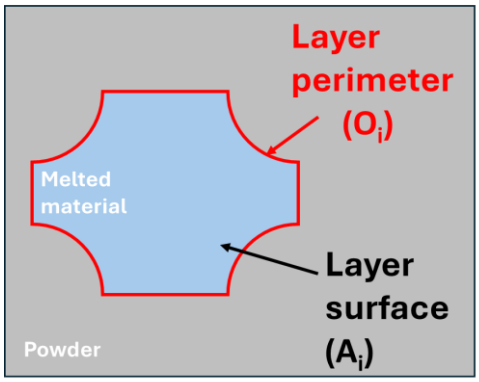

Figure 2.4: representation of the elements necessary for calculating the KPI: Powder to layer surface

The parameters in the formulas are reported in Table 2.4.

Table 2.4: parameter for the formulation of the KPIs

parameter	Description
A	Surface of the layer
O	Perimeter of the layer
$f \in \mathbb{N}$	Branch index
$i \in \mathbb{N}$	Layer index
$N \in \mathbb{N}$	Total amount of layers
a	Surface of a branch
$b_i \in \mathbb{N}$	Number of branches per layer
$c_i \in \mathbb{N}$	Number of contour vector block per layer
z_i	Height of the layer i
V_i	Volume of the layer i

The KPIs are calculated on the same orientations which are considered for the thermal simulation.

2.5 Calculation of the overall KPI

To complete the algorithm for ranking different orientations, two optimization approaches are employed. The first optimization investigates the correlation between the thermal simulations and the KPIs, while the second optimization aims to predict deformation and rank the orientations. To compare the results obtained with the thermal simulations performed using Ansys Additive with the KPIs, the Spearman factor (ρ) is utilized. This nonparametric measure assesses the monotonic relationship between two variables by comparing their ranks, evaluating how well the correlation can be described by a monotonic function. The Spearman coefficient is calculated using the following equation:

$$\rho = 1 - \frac{6 \sum d_i^2}{n(n^2 - 1)} \tag{2.8}$$

Where:

d_i: is the different between ranks

n: is the number of tests/ measurements

The goal of the optimization is to create an overall KPI which will be used to do the rating of the orientations. This overall KPI is a linear combination of the six KPIs that are been presented earlier. The coefficients of the combination are called weights w_i. The objective is to maximize the Spearman factor and consequently the correlation between the deformation and the overall KPI by modifying the weights in the proper way.

$$KPI_{Overall} = \sum w_i \, KPI_i \tag{2.9}$$

Where:

- w_i: is the generic weight
- KPI_i: is the generic KPI

Consequently, the objective function of the optimization, which is the Spearman factor.

$$F(x) = \rho$$

Moreover, the optimization is constrained: each weight must be between 0 and 1 and the summatory of the weights must be equal to one:

$$0 \leq w_i \leq 1$$

$$\sum_{i=1}^{n} w_i = 1 \tag{2.10}$$

Where:

- w_i: is the generic weights
- n: is the number of KPIs

Two optimizations are performed for each part. The first optimization aims to assess whether the overall KPI accurately represents the deformation observed across the different orientations. To achieve this, the parts are examined individually. The weights are modified to guarantee the best correlation between the KPIs calculated on the part under examination and its deformations. This section during the study is called Correlation.

The other optimization aims to determine if it is possible to use the overall KPI to evaluate different orientations of a part where the deformations are unknown. To do this, it is initially assumed that the parts is not analysed through thermal simulations, meaning

the deformations are unknown, but the KPIs are still calculated. The weights required to calculate the overall KPI are not obtained following the previous framework. Instead, in this case, the weights are derived by maximizing the sum of the Spearman correlation factors for the other seven known parts. Specifically, the goal is to maximize the correlation between the deformations and the KPIs of these seven parts. These parts are subjected to thermal simulations, so their deformations are known. The weights are then combined with the geometric KPIs calculated for the part under consideration to determine the overall KPI. This process is repeated for all eight parts included in the analysis. For results analysis, the correlation between the overall KPI and actual deformations of the part is measured. This process is referred to as Transferability. The procedure is schematized in Figure 2.5.

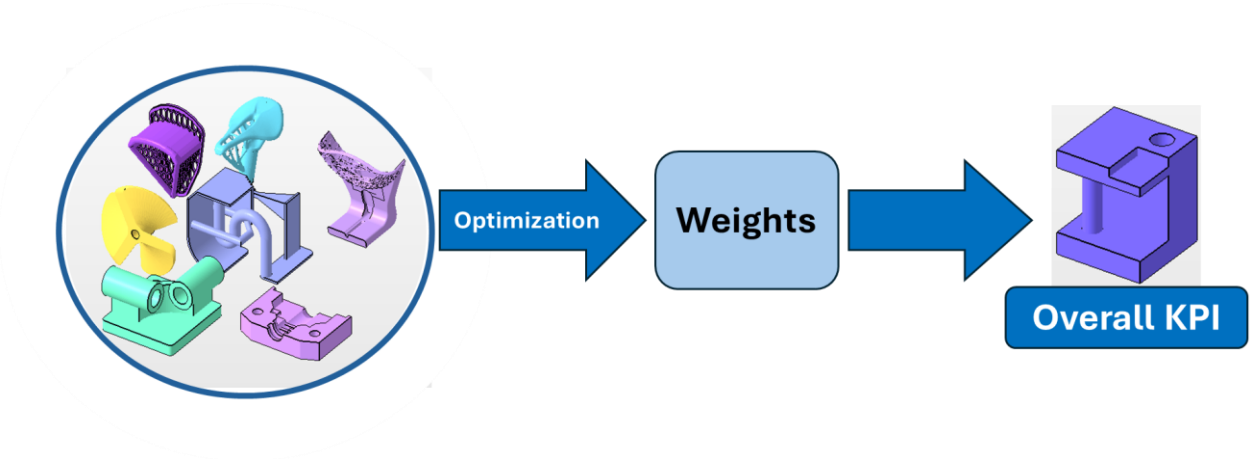

Figure 2.5: schematization of the process to calculate the Overall KPI

To determine the degree of correlation between the two variables, Cohen's standard is used:

- $|\rho| \geq 0{,}5$: the correlation is considered relevant
- $0{,}3 \leq |\rho| < 0{,}5$: the correlation is considered moderate
- $0{,}1 \leq |\rho| < 0{,}3$: the correlation is considered weak

2.6 Results of the thermal simulations

This chapter presents the results of the thermal simulations. The simulations provide the deformations calculated for each part, with an example of part 4 shown in Figure 2.6. Additionally, the displacement of each voxel layer caused by the printing process is obtained and it is divided into its three components along the X, Y and Z axes.

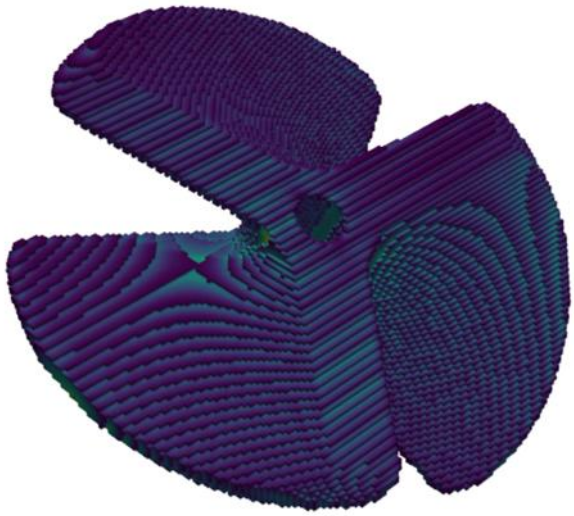

Figure 2.6: example of the outcome of the simulation with Ansys (Part-ID 4)

Figure 2.7: average, maximum and minimum displacement of each orientation of each part obtain from the thermal simulations reports the results of the average total displacement, the maximum and minimum total displacements for each orientation of each part.

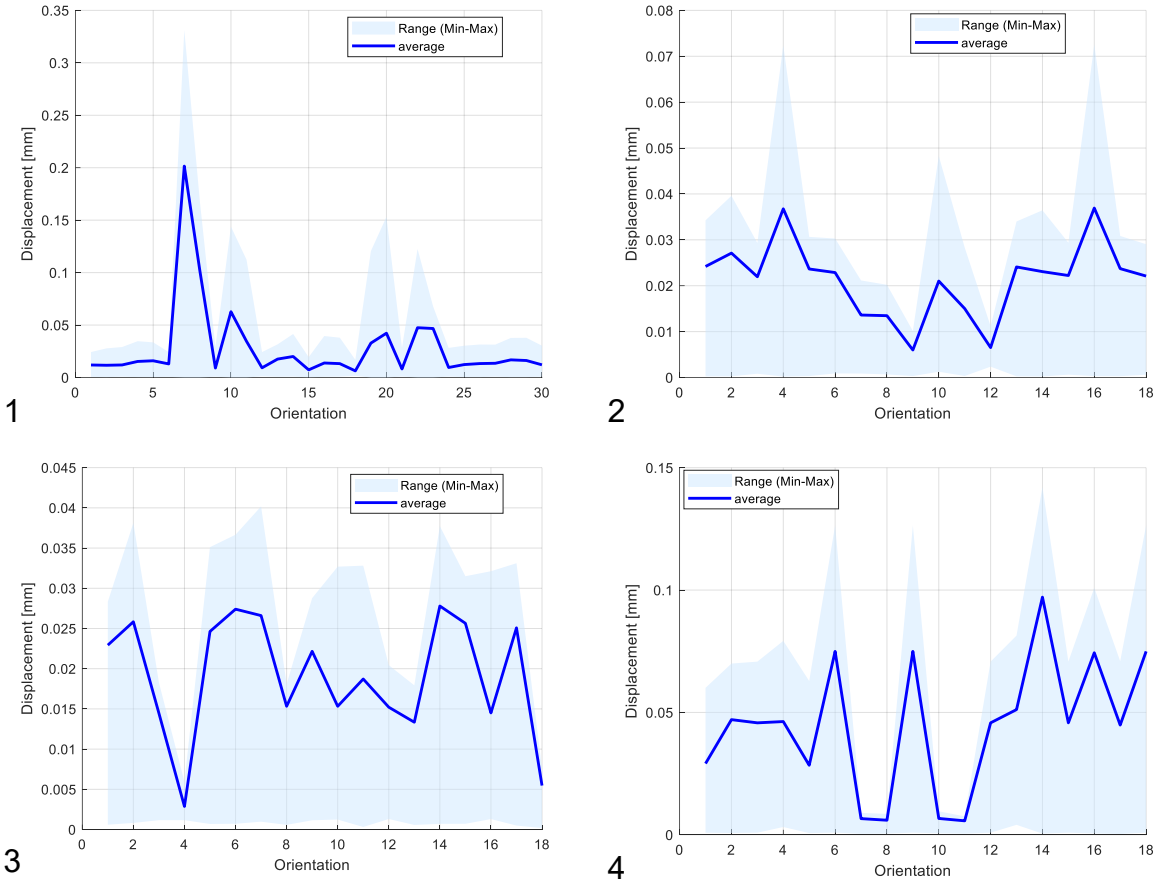

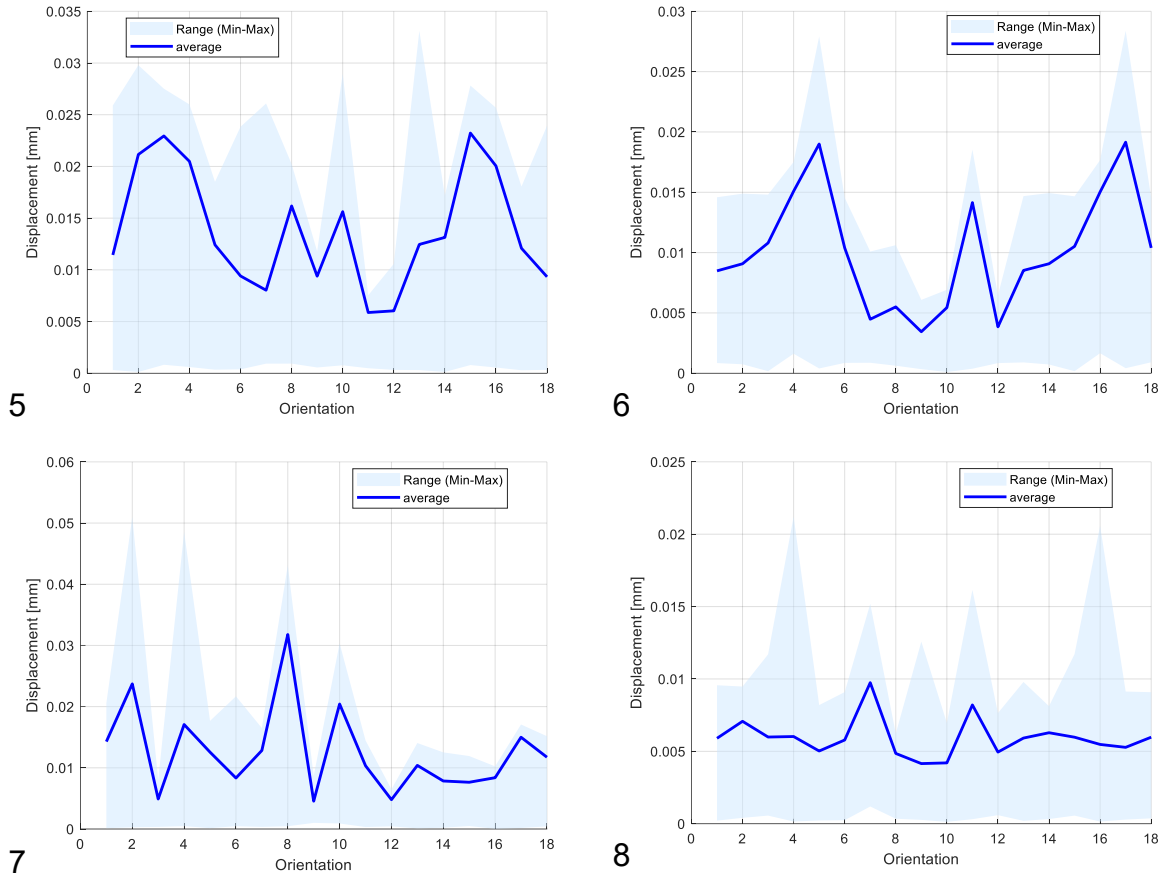

Figure 2.7: average, maximum and minimum displacement of each orientation of each part obtain from the thermal simulations

2.7 Optimization and results

In this section, the results that are obtained in terms of correlation between the KPIs and the deformations calculated with the thermal analyses are presented, in this phase the aim is to maximize the correlation between the overall KPI and the results from the thermal simulations. The results are shown both in terms of correlation and transferability. The figure shows the Spearman factor calculated between the deformation trend and the KPIs trend for the orientations considered. The comparison is made for each of the parts between the Transferability and the Correlation and it is illustrated in Figure 2.8.

Figure 2.8: difference of the values of the Spearman factor between correlation and transferability

Analysing the results, the Correlation can be summarized as follows:

- 3 parts shows a non-significant correlation (part-ID 1, 4, 8)
- 2 parts show a moderate correlation (part-ID 3, 6)
- 3 parts shows a significant correlation (part-ID 2, 5, 7)

The results, obtained with the optimization of the weights, reveals an average correlation of 0,389. This corresponds to a moderate correlation.

While for the Transferability the results are:

- 1 part shows a relevant correlation (part-ID 7)
- 1 part shows a moderate correlation (part-ID 2)
- 6 parts show a non-significant correlation (part-ID 1, 3, 5) or inverse correlation (part-ID 4, 6, 8)

This process guarantees an average Spearman factor equal to 0,00735. This corresponds to a non-significant correlation.

Comparing the results of Correlation and Transferability. It is evident a worsening of the transferability results as expected for the data transfer process to assess the necessary orientation in the algorithm. The decrease of the average Spearman factor is

equal to 0,382. Moreover, the parts with at least a moderate correlation are reduced from five to two (part-ID 2, 7), which are the parts with the best correlation in the first step.

An analysis of the results regarding the influence of various geometric features indicates that they are comparable across the two studies. Indeed, in both the features: transition thin to massive, edges, walls and pipes are within the range of one standard deviation from the mean. Instead, they go to deviate below this range for the features: Grids. This suggests a negative impact of this feature in the results obtained.

Regarding the influence of the complexity of the analysed geometry, different results were obtained. in the correlation study, the complexity generates a large spread in the data on the Spearman factor, this suggests a non-significant effect of the complexity. In contrast, in the transferability a tendency to worsen the results was obtained with the increase of the surface to volume ratio. this indicates a negative effect of the complexity on the results.

2.8 Discussion of the RWTH algorithm

The study demonstrates promising results regarding the correlation between the overall KPI and the deformation obtained from the simulations, with a moderate correlation observed on average across the parts. Specifically, 63% of the tested parts exhibit at least a moderate correlation and 38% show a relevant correlation. However, the analysis of the prediction of the deformation, using the transferred weights, reveals that on average the models does not guarantee reliable results, indeed the average correlation revealed is not significant.

This problem is analysed by focusing on the results for the weights of the single KPI, with Figure 2.9, it becomes evident that there is a strong predominance on one single KPI. Indeed, the KPI downskin surface has an average weight from the optimization for each part of 0,76. On the other side, the effect of the KPIs massiveness and branch surface ratio is almost negligible. The remain influence is subdivided almost equally between the other 3 KPIs: amounts of branches, contour-vector and powder to layer surface.

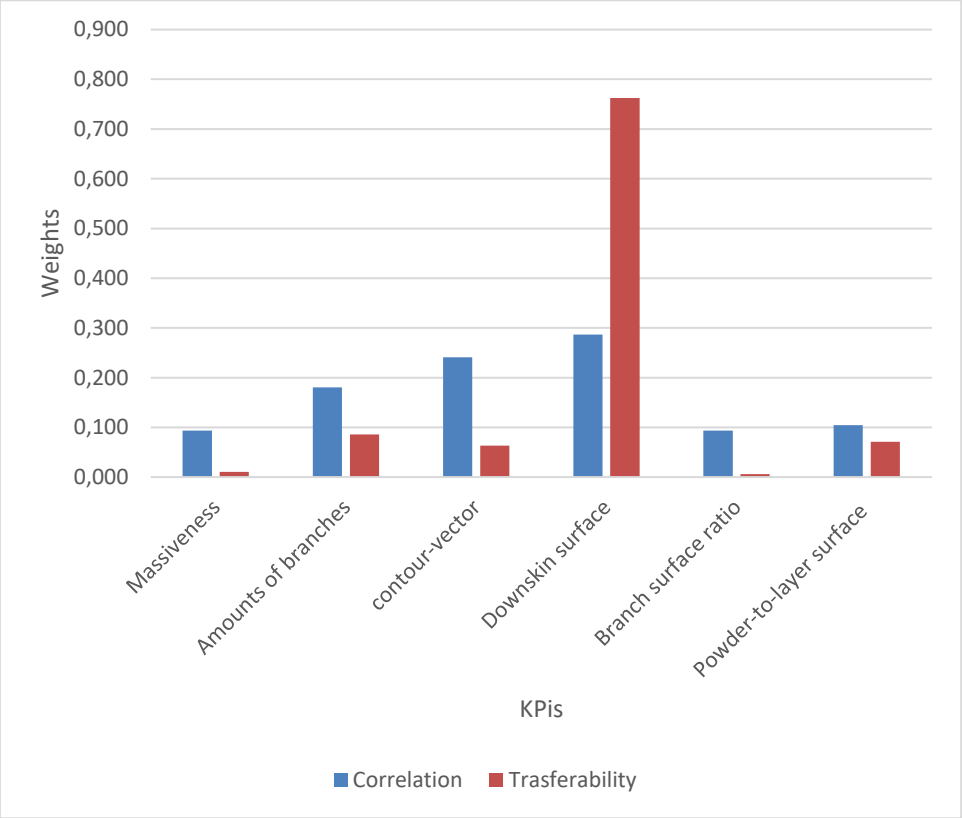

Figure 2.9: comparison of the weights of each KPI from the correlation and transferability analysis

Table 2.5: comparison of the average weight for each KPI

KPI	Weights of correlation	Weights of transferability	Differences of weight
Massiveness	0,094	0,011	0,083
Amounts of branches	0,181	0,086	0,095
Contour-vector	0,241	0,064	0,177
Downskin surface	0,287	0,763	-0,476
Branch surface ratio	0,093	0,006	0,087
Powder-to-layer surface	0,105	0,071	0,034

The relevance of the downskin surface KPI leads to problems in terms of applicability of the model. Indeed, with a preponderant impact of a single KPI, there will be a tendency to have a model that performs better in the components where the single KPI has good results. In contrast, if the KPI downskin surface does not guarantee good correlation, you will have an ineffective model. In this way, the model will be unstable in its performance.

To develop a more robust model with stable and precise results across all parts and to mitigate the influence of outlier results, an increased number of analysed parts is required. Expanding the number of data would enhance the statistical reliability of the findings and reduce variability caused by unique characteristics of individual parts. Furthermore, incorporating parts with single diverse geometries and features would improve the model's generalizability, ensuring its applicability across a wider range of scenarios.

The study confirms the literature findings regarding the downskin surface. Indeed, this surface has a significant impact on the onset of deformations, as shown by the weight analysis during the optimizations in Figure 2.9. Regarding the branches and variations in geometry, significant results were observed, as expected from the literature, particularly in the correlation analysis. However, their relevance significantly decreased in the transferability phase. Specifically, for the branches, a greater importance was observed in the number of branches rather than their geometry. The massiveness and the influence of the powder to the layer surface demonstrate outcomes not aligned with the literature.

To have a better overall vision, the results are analysed in terms of Spearman factor between the deformations and the downskin surface KPI, as reported in Figure 2.10.

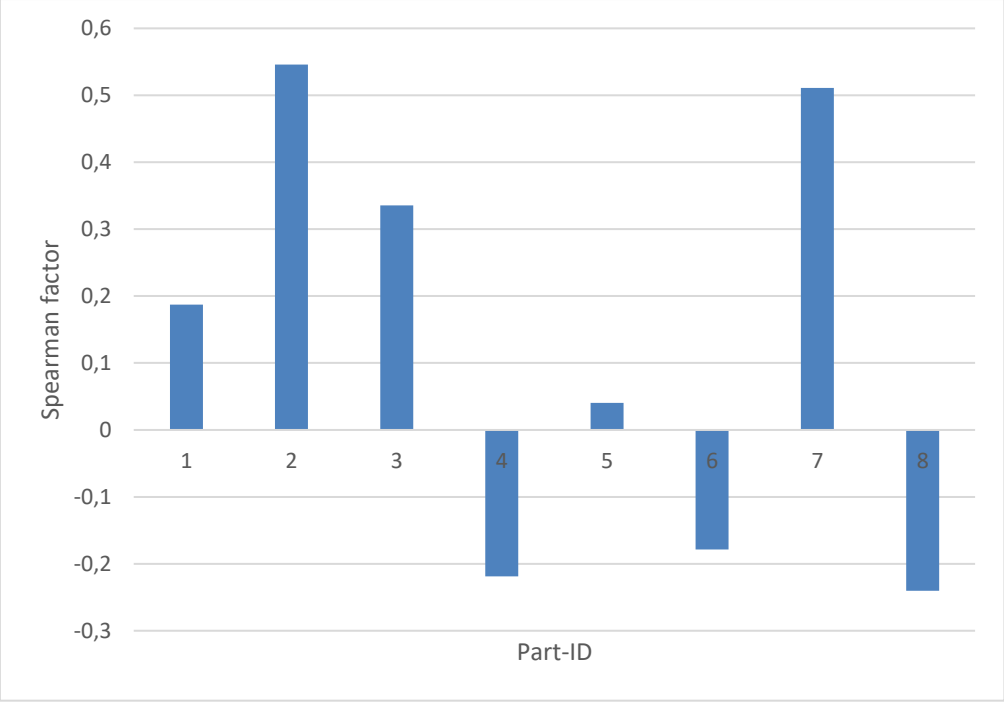

Figure 2.10: correlation measured with Spearman factor between deformations and KPI downskin in each single part

The image confirms the relationship between the good results obtained from the downskin surface KPI and those from the optimization of transferability. Indeed, all the parts with an inverse correlation with the downskin surface KPI (part-ID 4, 6 and 8) also present an inverse correlation with the overall KPI for orientation ratings. Furthermore, even the parts that have the best in terms of transferability (part-ID 2 and 7) are also the two best in terms of Spearman factor values with the downskin surface KPI.

This analysis confirms the strengths and weaknesses of the model linked to its dependence to the downskin surface KPI, which limits its replicability.

3 Comparison: Netfabb and RWTH algorithm

In this chapter, the results of orientation optimization performed using *Netfabb* and the algorithm developed at RWTH Aachen University are analysed and compared.

The comparison was conducted using the same set of parts that were employed in the development of the RWTH Aachen University optimization model. For the *Netfabb* optimization, the default parameter weights were used. All other relevant parameters used in the comparison are summarized in Table 3.1.

Table 3.1: Netfabb parameters for the optimization of the orientation

Parameters	**values**
Critical angle(Di Wang et al. 2013)	45°
Smallest rotation between	10°
Precise volume	X

The analysis considers not only the overall optimal build orientations but also those considered optimal with respect to each individual optimization parameter.

For the results obtained using the RWTH Aachen University algorithm, both optimal orientations identified through the transferability and correlation methods are included in the evaluation, provided they differ. Each part is examined individually to ensure a detailed and component-specific comparison.

3.1 Part 1

From the results of the optimization of the orientation with Netfabb the best overall orientation reported in Figure 3.1.

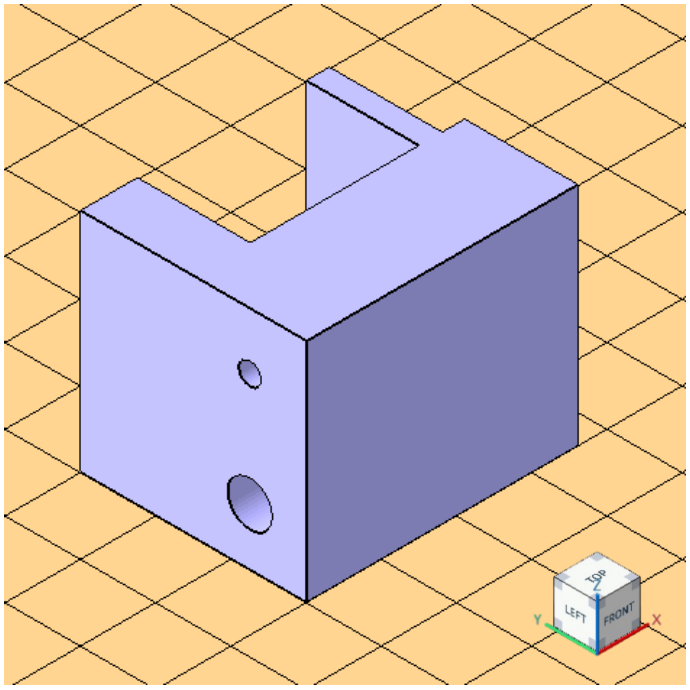

Figure 3.1: Part 1 best overall orientation with Netfabb

The best orientation for each of the parameter are reported in the Figure 3.2.

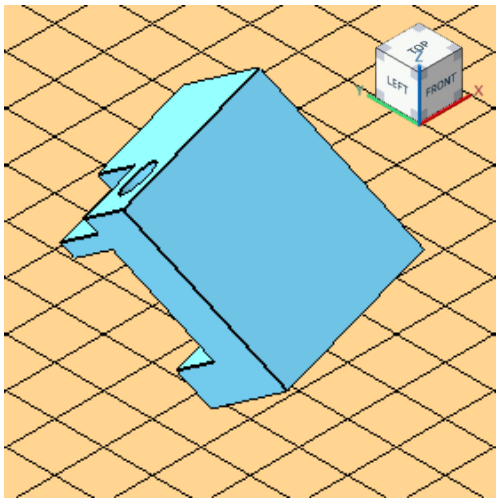

a. Supported area

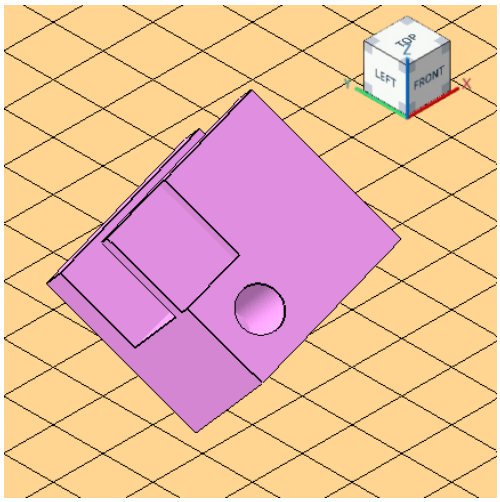

b. Supported volume

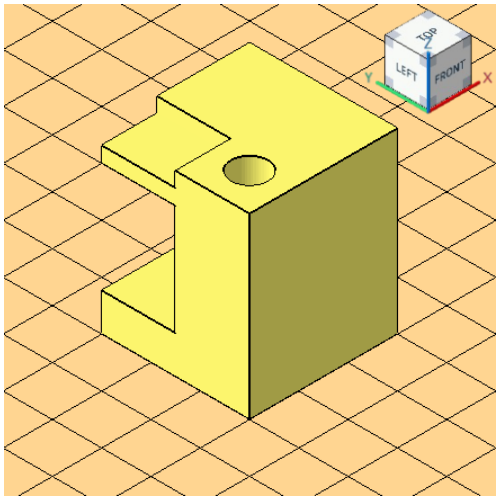

c. Bounding box volume

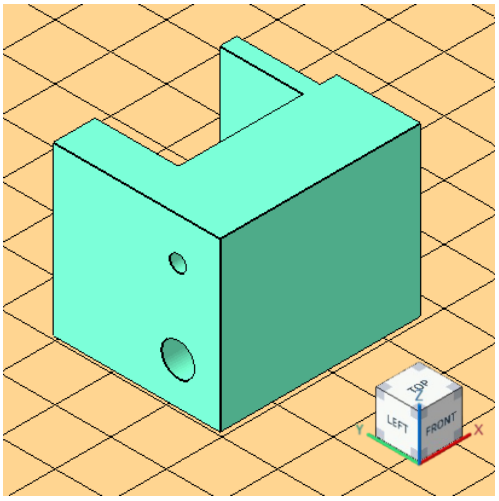

d. Height

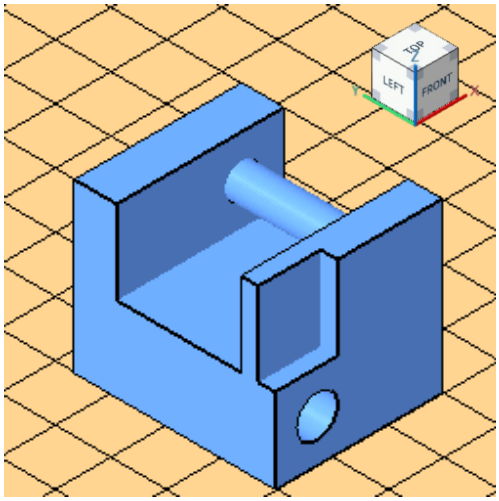

e. Center of gravity

Figure 3.2: Part 1: best orientation for each parameter with Netfabb

The outcomes of the orientation optimization method developed at RWTH Aachen University are presented, including both the correlation and transferability analyses. The results of these two studies are illustrated in Figure 3.3.

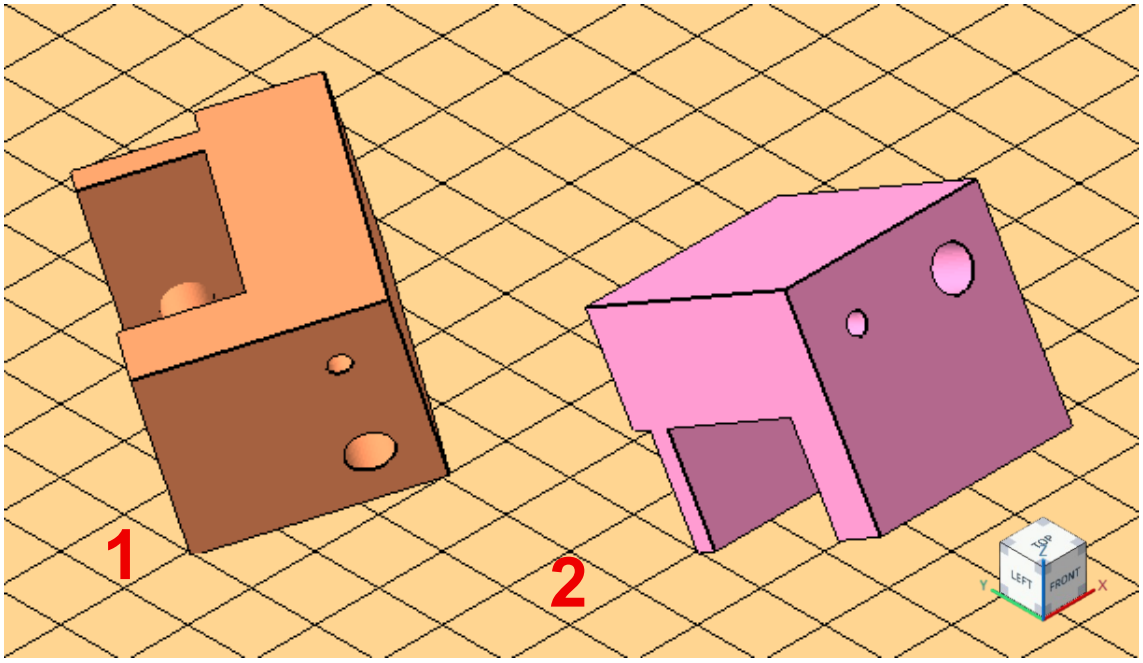

Figure 3.3: Part 1: best orientation with RWTH method: 1 Correlation, 2 Transferability

In this case, the orientation assessed using Netfabb is primarily influenced by the parameters of part height and center of gravity. Specifically, the selected orientation aligns with the optimization of part height and also produces favourable results with respect to the center of gravity. However, this orientation introduces certain drawbacks, notably the necessity for internal support structures within the channels. These supports complicate post-processing and removal, contribute to increased surface roughness. This orientation has extensive cross-sectional areas that must be scanned in each layer. These factors collectively increase the risk of deformation during fabrication.

Conversely, the orientation generated by the algorithm developed at RWTH does not prioritize optimization of the height or center of gravity. While this may negatively affect thermal diffusion through the build plate, the RWTH orientation avoids the formation of large scan areas per layer, thereby potentially improving thermal management and reducing the likelihood of deformation.

In summary, the orientation proposed by Netfabb adheres to general guidelines commonly applied in additive manufacturing. In contrast, the RWTH approach offers a more targeted strategy, emphasizing specific design and process considerations over generalized optimization criteria.

The results are summarized in the Table 3.2:

Table 3.2: Part 1: comparative overview of advantages and disadvantages of the methods

Netfabb		**RWTH**	
Advantages	**Disadvantages**	**Advantages**	**Disadvantages**
Low height	Supports in inner channels	Thermal management	Height
Low center of gravity	Thermal management	Supports	Center of gravity

3.2 Part 2

Based on the orientation optimization results obtained using Netfabb the best overall orientation reported in Figure 3.4.

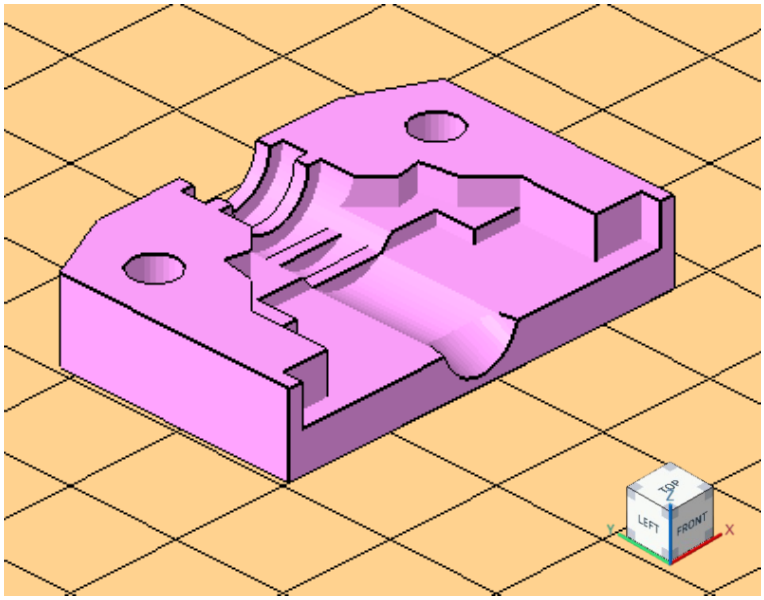

Figure 3.4: Part 2: best overall orientation with Netfabb

Figure 3.5 presents the optimal orientation for each evaluated parameter.

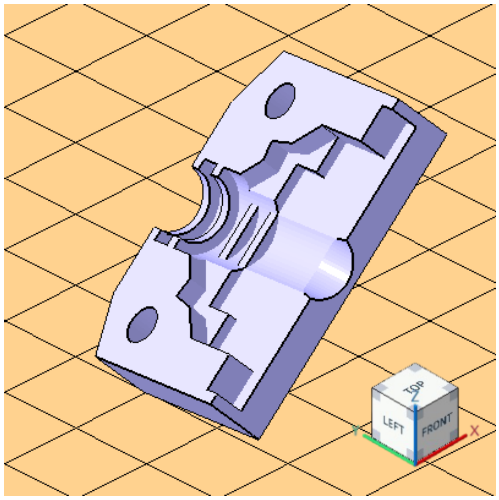

a. Supported area

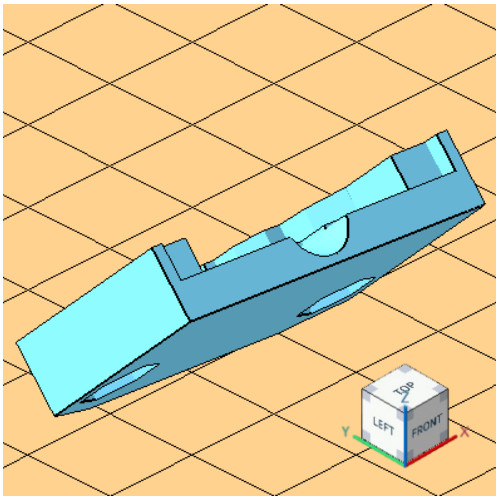

b. Supported volume

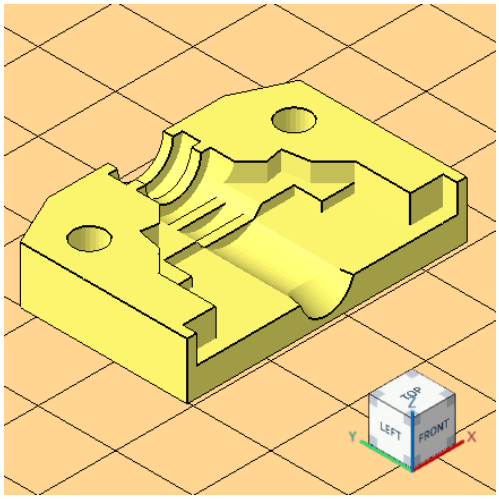

c. Bounding box volume

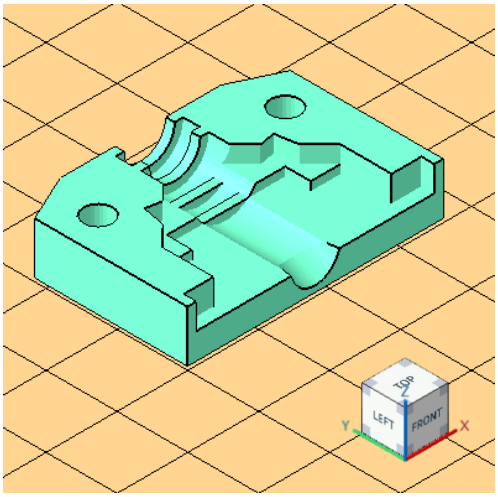

d. Height

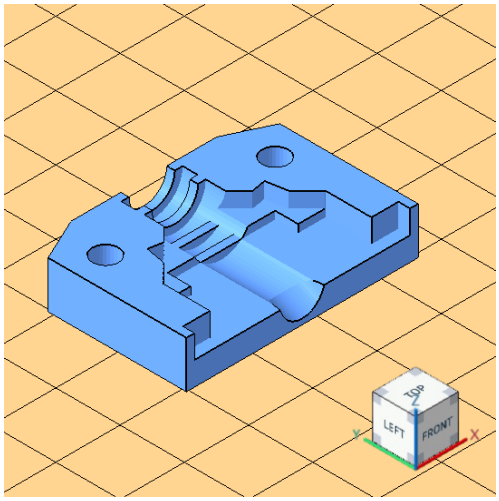

e. Center of gravity

Figure 3.5: Part 2: best orientation for each parameter with Netfabb

The results of the orientation optimization approach proposed by RWTH Aachen University are reported, with a focus on both the correlation analysis and the transferability study. These findings are visualized in Figure 3.6.

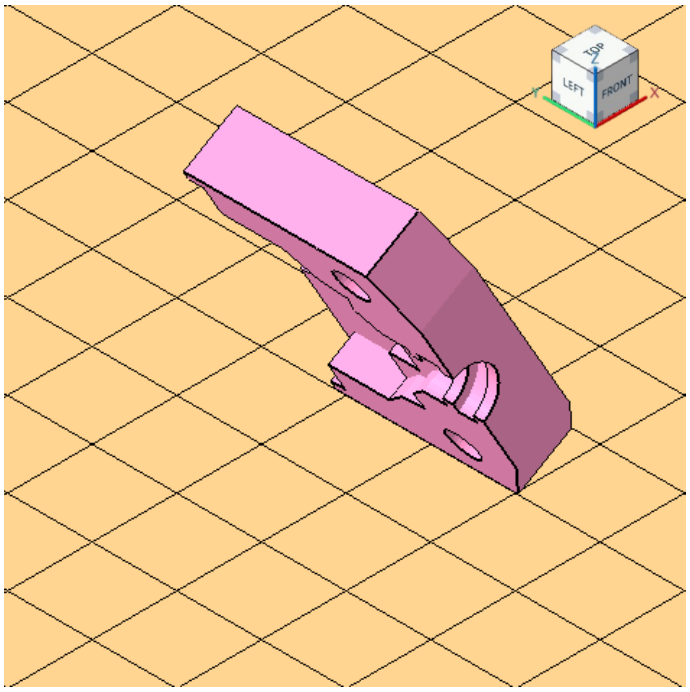

Figure 3.6: Part 2: best orientation with RWTH method: correlation and transferability coincide

Also, this the case the considerations are similar to the previous one, indeed Netfabb chooses an orientation focusing mainly on the minimization of the height, the center of gravity and the bounding box volume. The downward aspects are also similar; indeed, the orientation present the biggest possible surface of scanned area and sudden and impactful variance on the scanned area, these aspects are related with high residual tension and deformation. The presence of support structures is related only to the connection with the base plate.

The RWTH method introduces the necessity of support structures in the holes, the detail is report in Figure 3.7, which is an additional step in the post-processing process, the presence of other supports is limited to the smallest face of the part. This orientation exhibits smaller and more gradual variations in scanned surface area compared to that generated by Netfabb. On average, as well as at peak values, the total scanned area is significantly reduced. However, the printing process requires more time due to the build height.

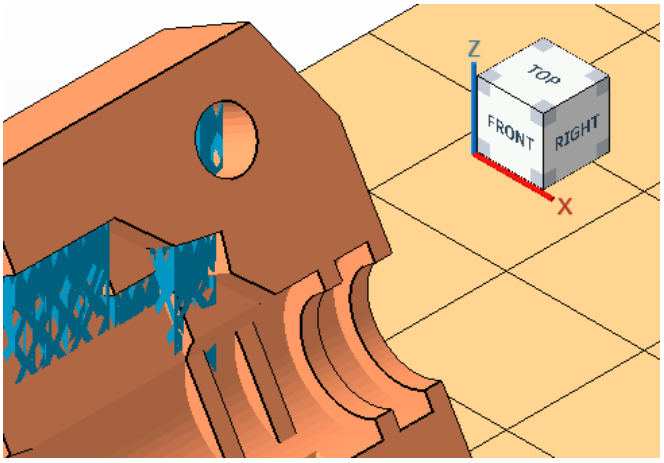

Figure 3.7: detail of the support structure

Netfabb optimizes the orientation to minimize the build time and limit the use of support structures. In contrast, the RWTH approach suggests an orientation which is focused on reducing the residual stress and thermal deformation which are typical of this technology.

The results are summarized in Table 3.3:

Table 3.3: Part 2: comparative overview of advantages and disadvantages of the methods

Netfabb		**RWTH**	
Advantages	**Disadvantages**	**Advantages**	**Disadvantages**
Low height	Thermal management	Thermal management	Height
Low center of gravity			Center of gravity
			Supports in inner channels

3.3 Part 3

The optimal part orientation, as determined through the orientation optimization module in Netfabb, is illustrated in Figure 3.8.

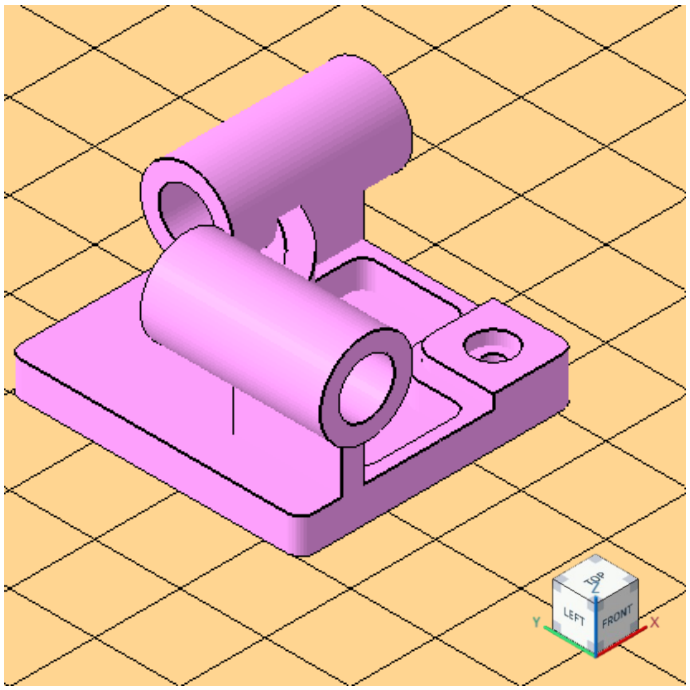

Figure 3.8: Part 3: best overall orientation with Netfabb

The best orientation corresponding to each parameter is reported in Figure 3.9.

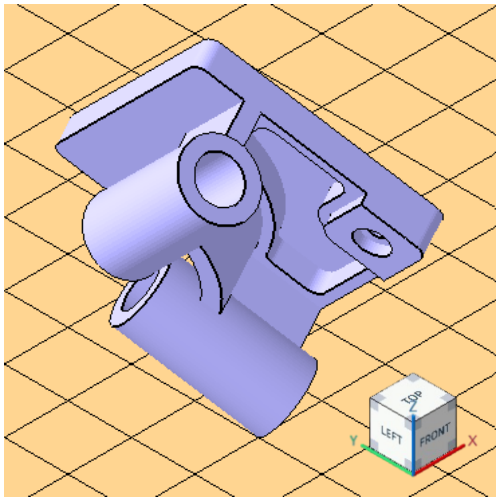

a. Supported area

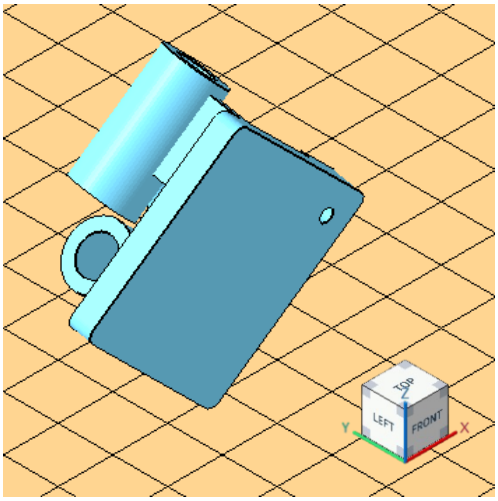

b. Supported volume

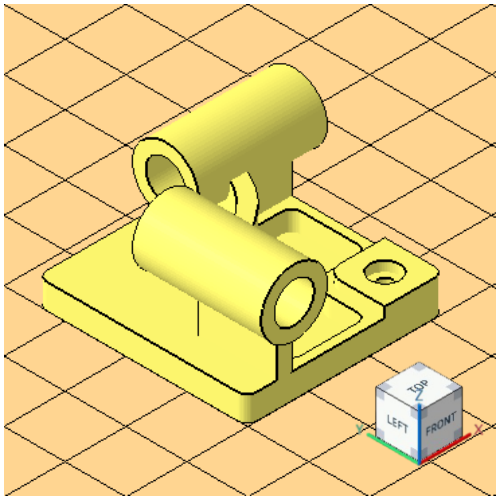

c. Bounding box volume

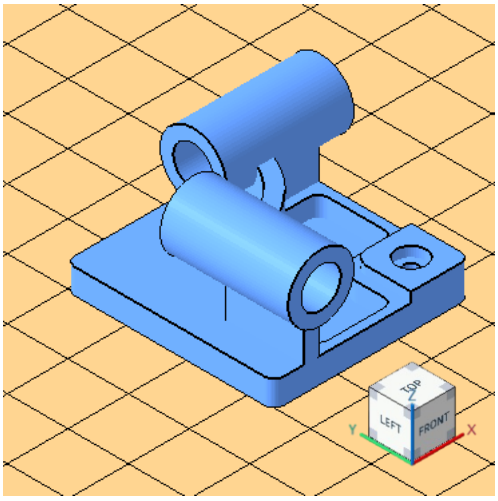

d. Height

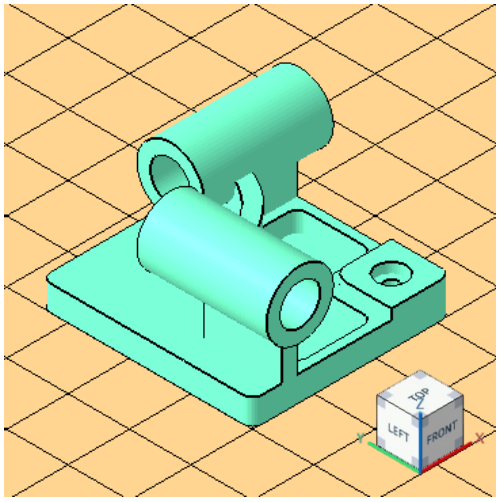

e. Center of gravity

Figure 3.9: Part 3: best orientation for each parameter with Netfabb

The outcomes of the orientation optimization method developed at RWTH Aachen University are presented, including both the correlation and transferability analyses. The results of these two studies are illustrated in Figure 3.10

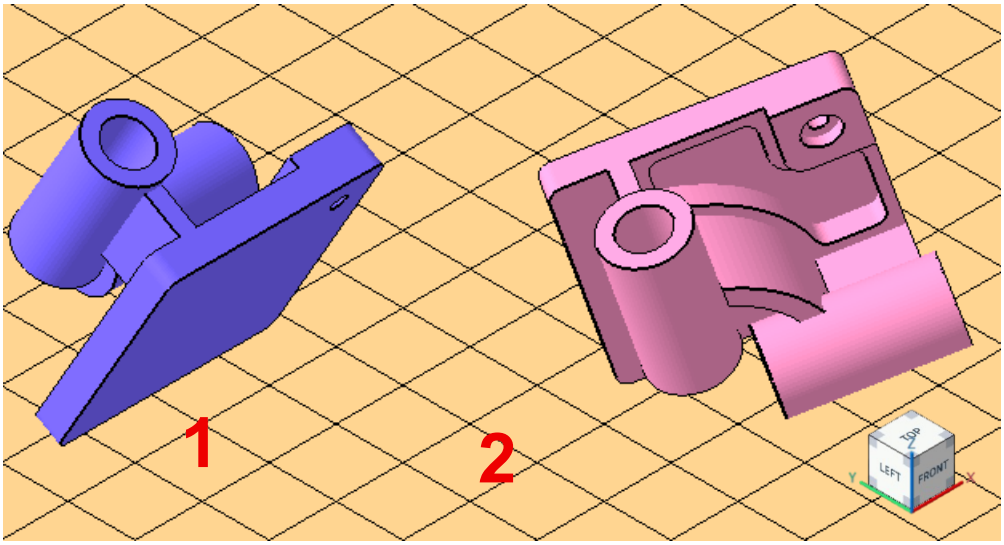

Figure 3.10: Part 3: best orientation with RWTH method: 1 Correlation, 2 Transferability

Consistent with earlier observations, the solutions provided by the two methods differ. The Netfabb approach predetermines key parameters: Bounding box volume, height and center of gravity. This guarantees good performance in terms of building time and stability, the support structures are used to sustain the channels.

The solution proposed by RWTH has some analogies with the one suggested to minimize the support volume. Specifically, the support structure in one of the channels is no longer necessary, the comparison is shown in Figure 3.11, this is helpful also in the post processing, as it facilitates the removal of support material. Furthermore, large scan surface areas in the layers and abrupt variations in the scanned area were avoided to ensure process stability and reduce thermal stresses during fabrication.

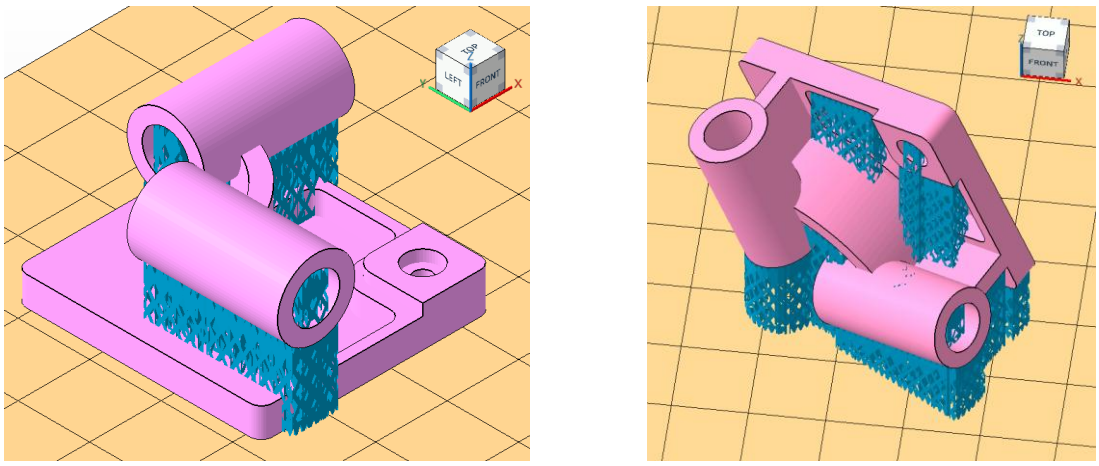

Figure 3.11: comparison of the support structures

The RWTH method results in a slower printing process, however it guarantees a point of view based on the specific technology, this potentially reduce the effect of thermal

cycles and consequently deformation and residual stress. Similar to the previous case Netfabb tends to prioritize the build time and the advantages of a large contact area with the base plate.

The results are summarized in the Table 3.4:

Table 3.4: Part 3: comparative overview of advantages and disadvantages of the methods

Netfabb		**RWTH**	
Advantages	**Disadvantages**	**Advantages**	**Disadvantages**
Low height	Supports in inner channels	Thermal management	Height
Low center of gravity	Thermal management	Supports	Center of gravity
Contact with base plate			

3.4 Part 4

From the results of the optimization of the orientation with *Netfabb* the best overall orientation reported in Figure 3.12.

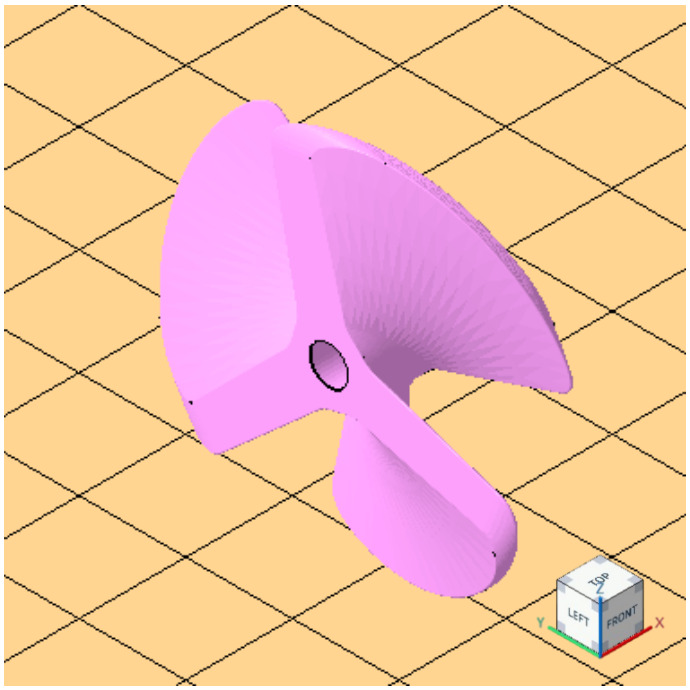

Figure 3.12: Part 4: best overall orientation with Netfabb

The best orientation corresponding to each parameter is reported in Figure 3.13.

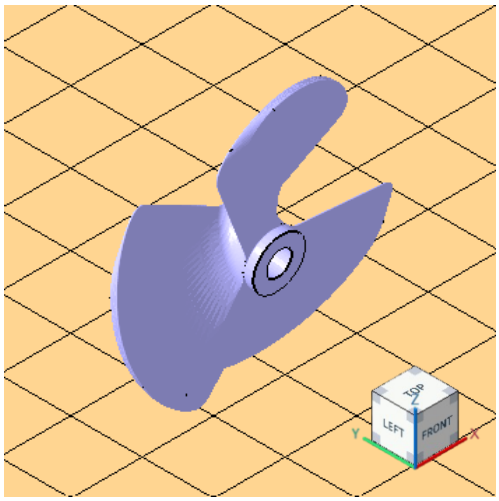

a. Supported area

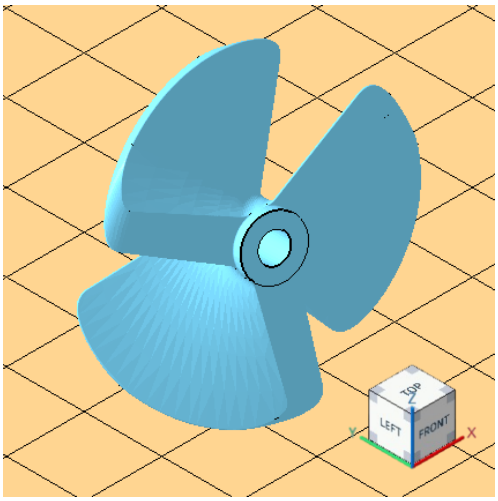

b. Supported volume

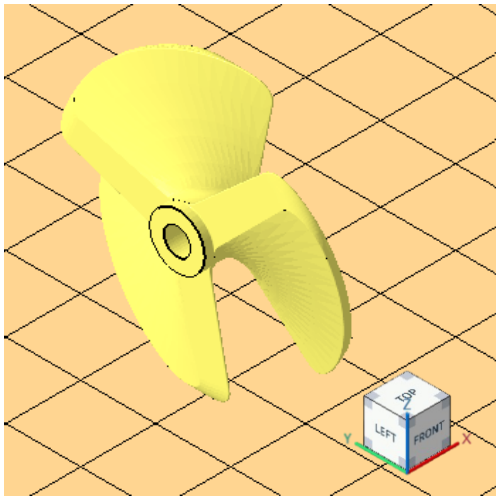

c. Bounding box volume

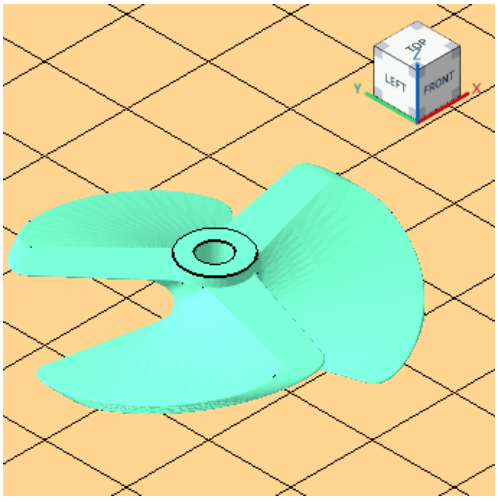

d. Height

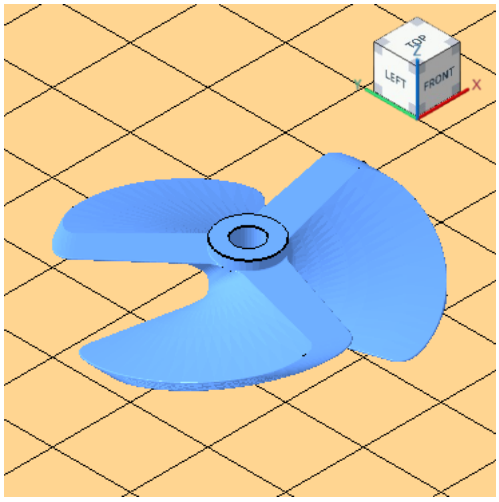

e. Center of gravity

Figure 3.13: Part 4: best orientation for each parameter with Netfabb

The results of the orientation optimization approach proposed by RWTH Aachen University are reported, with a focus on both the correlation analysis and the transferability study. These findings are visualized in Figure 3.14.

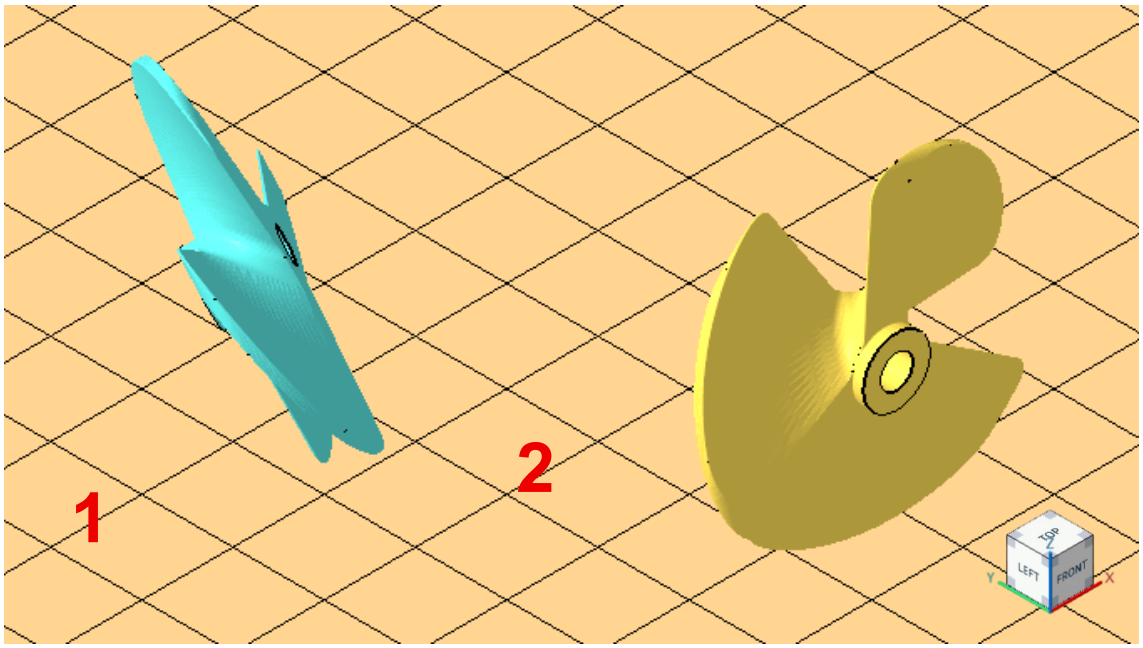

Figure 3.14: Part 4: Best orientation with RWTH method: 1 Correlation, 2 Transferability

The results for this part are similar, the orientations obtained using Netfabb and the transferability analysis being nearly coincident, a small rotation in the y-axes is present on the correlation results. These results optimise the volume and the area of support structures and the bounding box; this evidence is visible also in the results obtained for the related parameters. In this case the predominant factor for the Netfabb optimization is not related with the height and the center of gravity, this promotes an orientations that is slower than the optimum. However, it has a layer disposition that favours the thermal management and reduce the risk of thermal deformation. Moreover, the support structures are minimal in size and do not negatively impact the surface quality of the blades.

Consequently, it can be stated that both approaches prioritize print quality by enhancing thermal and material management, even if at the expense of printing speed.

The results are summarized in the Table 3.5:

Table 3.5: Part 4: comparative overview of advantages and disadvantages of the methods

Netfabb and RWTH	
Advantages	**Disadvantages**
Thermal management	Build time
Support structures	Height
	High center of gravity

3.5 Part 5

Figure 3.15 represents the best overall orientation identified through Netfabb's orientation optimization process.

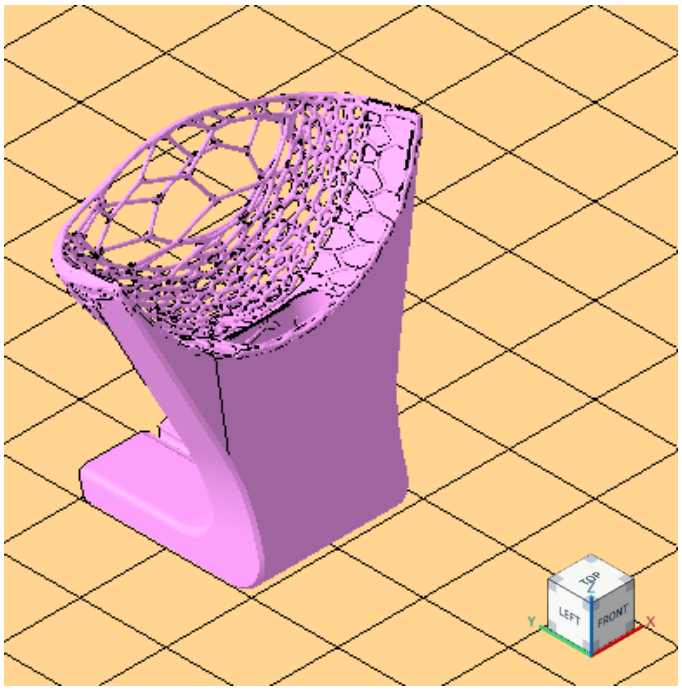

Figure 3.15: Part 5: best overall orientation with Netfabb

The best orientation corresponding to each parameter is reported in Figure 3.16.

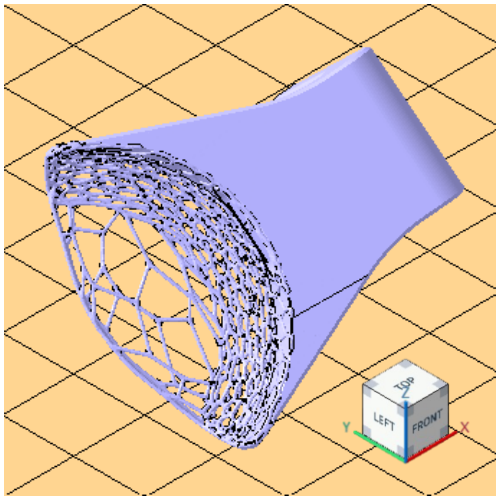

f. Supported area

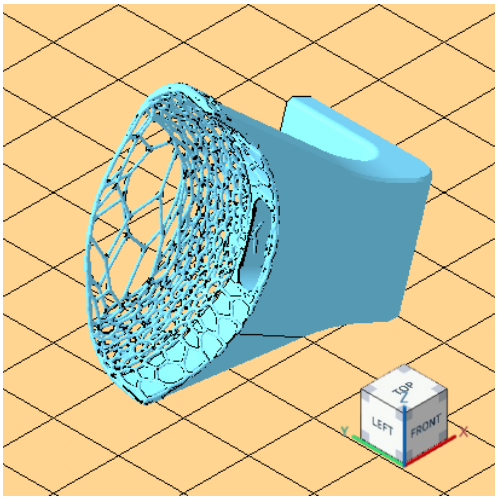

g. Supported volume

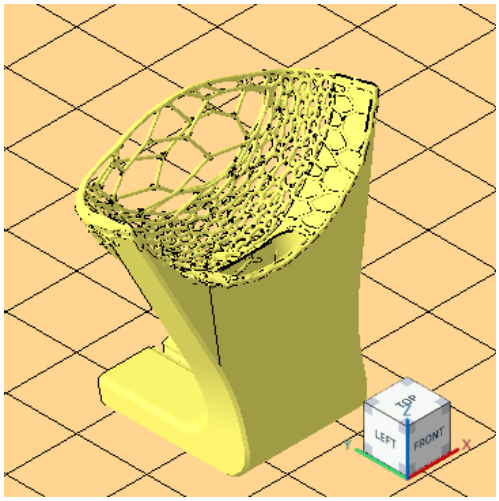

h. Bounding box volume

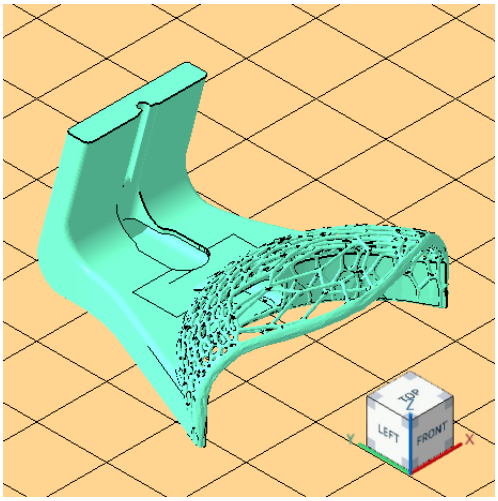

i. Height

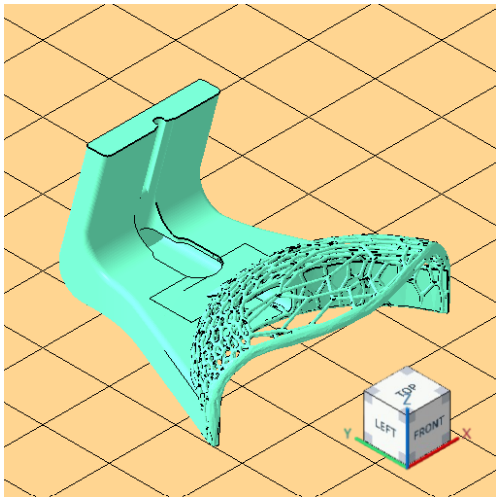

j. Center of gravity

Figure 3.16: Part 5: best orientation for each parameter with Netfabb

The outcomes of the orientation optimization method developed at RWTH Aachen University are presented, including both the correlation and transferability analyses. The results of these two studies are illustrated in Figure 3.17.

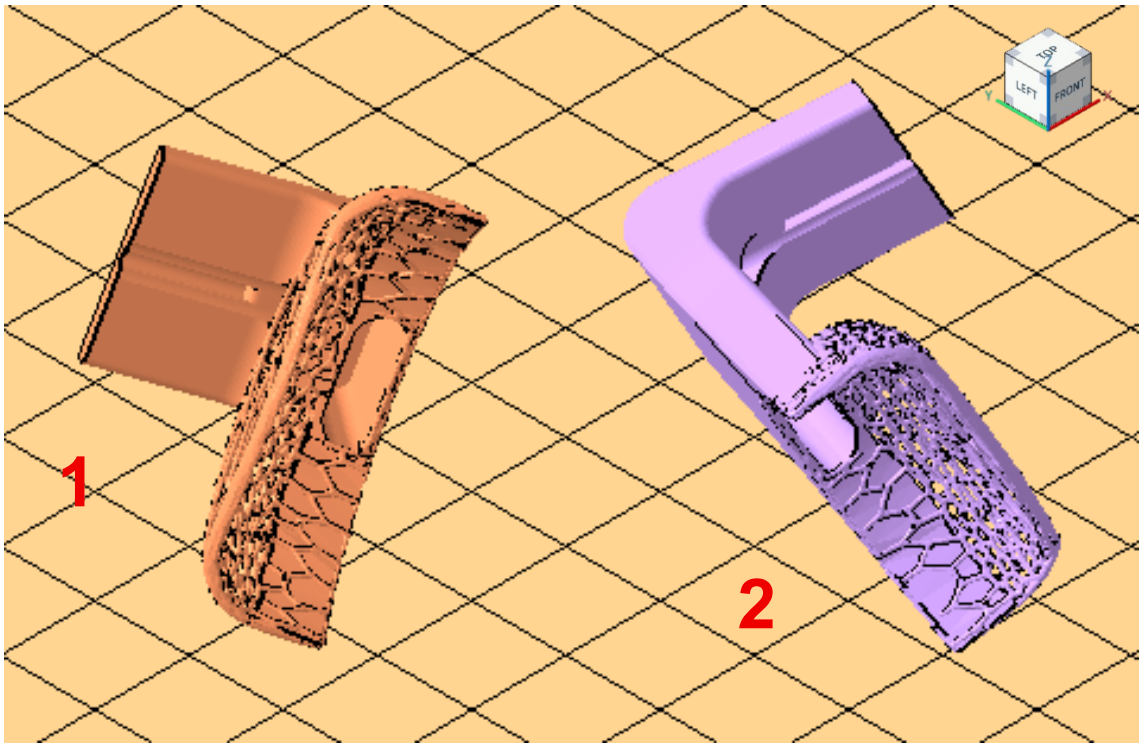

Figure 3.17: Part 5: Best orientation with RWTH method: 1 Correlation, 2 Transferability

For this part the presented solutions are discordant, Netfabb's orientation is the same that optimizes the parameter *Bounding box volume*, with a good trade-off between the other parameters.

On the other hand, the solution proposed by the RWTH method almost matches the solution that minimizes the parameters related to the support structures, specifically in the area where the geometry is thin and the removal of the supports can lead to component breakage. Indeed, it is comparable to solutions offered by Netfabb for the specific parameters related to the supports, this solution presents a reduced height according to the Netfabb orientation in favour of the build time. The comparison of the support structures is reported in Figure 3.18.

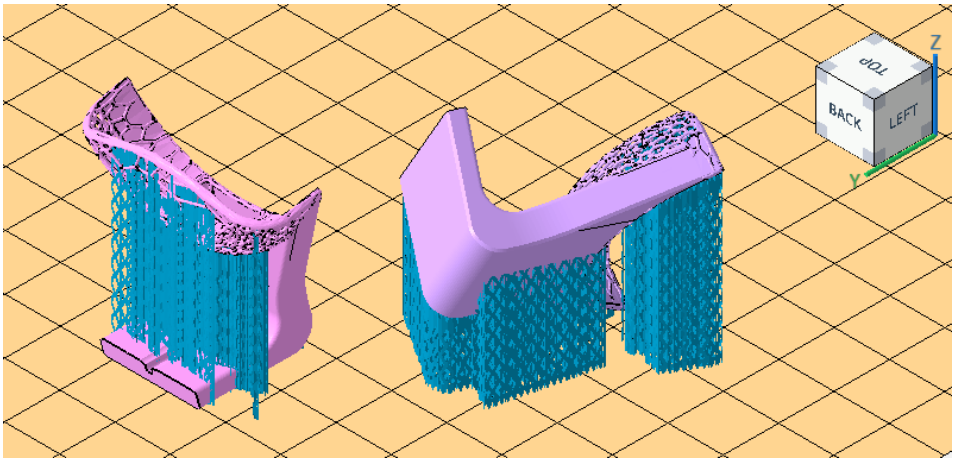

Figure 3.18: comparison of the support structures for the part 5

Among the solutions, none clearly outperforms the others in terms of thermal management and resulting deformations. However, the RWTH approach demonstrate improved optimization of support structures and build time.

The results are summarized in Table 3.6:

Table 3.6: Part 5: comparative overview of advantages and disadvantages of the methods

Netfabb		**RWTH**	
Advantages	**Disadvantages**	**Advantages**	**Disadvantages**
Bounding box volume	Supports	Supports	Bounding box volume
	Supports in thin section	Supports in thin section	
		Height	

3.6 Part 6

From the results of the optimization of the orientation with Netfabb the best overall orientation reported in Figure 3.19.

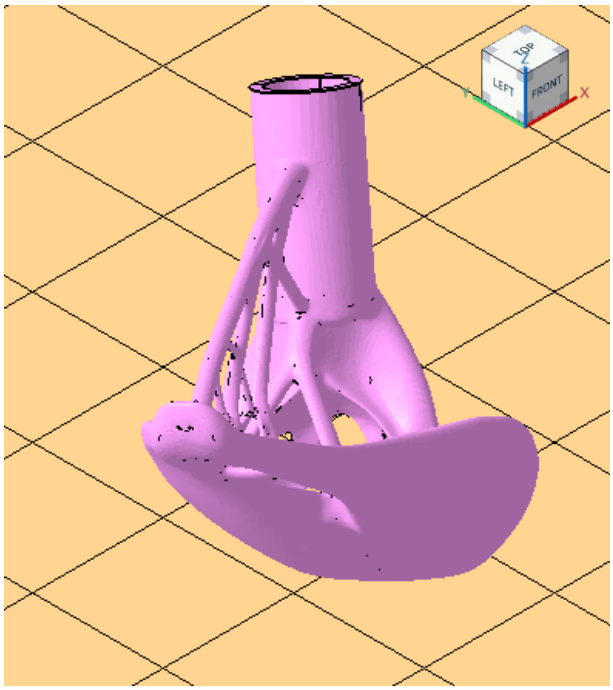

Figure 3.19: Part 6: best overall orientation with Netfabb

The optimal orientation for each parameter is shown in Figure 3.20.

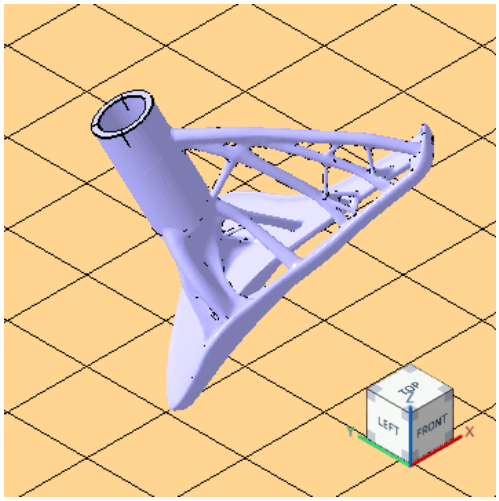

a. Supported area

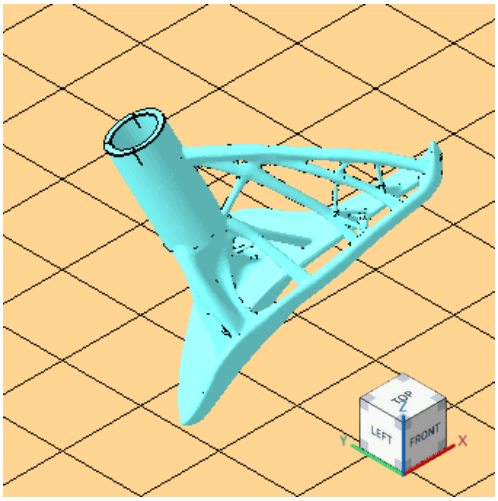

b. Supported volume

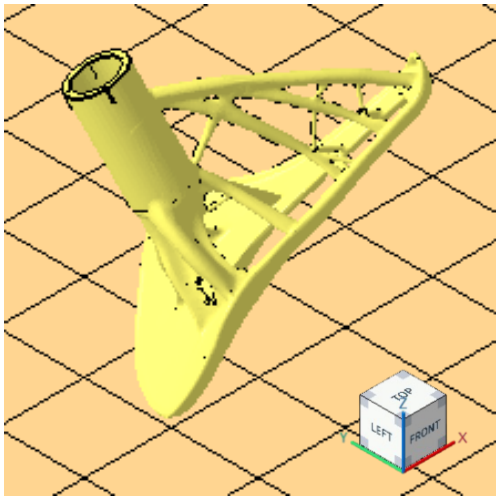

c. Bounding box volume

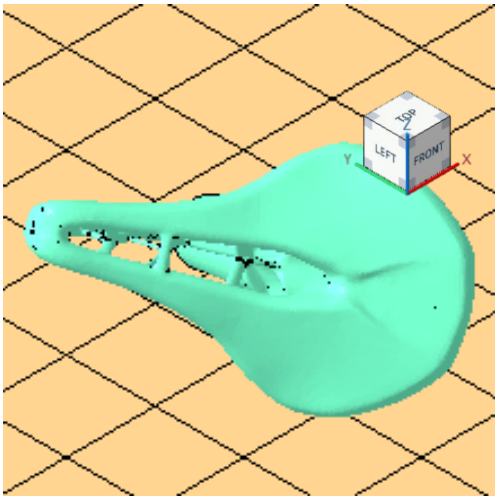

d. Height

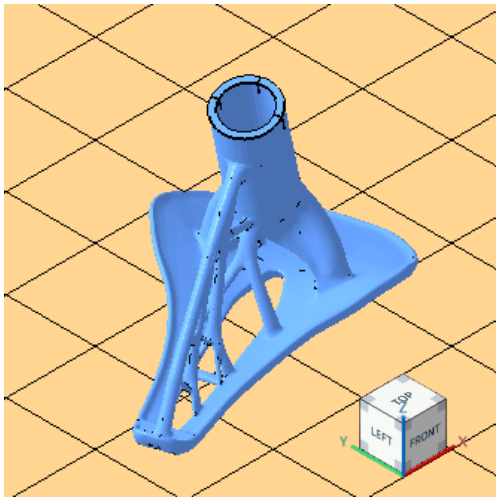

e. Center of gravity

Figure 3.20: Part 6: best orientation for each parameter with Netfabb

The results of the orientation optimization approach proposed by RWTH Aachen University are reported, with a focus on both the correlation analysis and the transferability study. These findings are visualized in Figure 3.21.

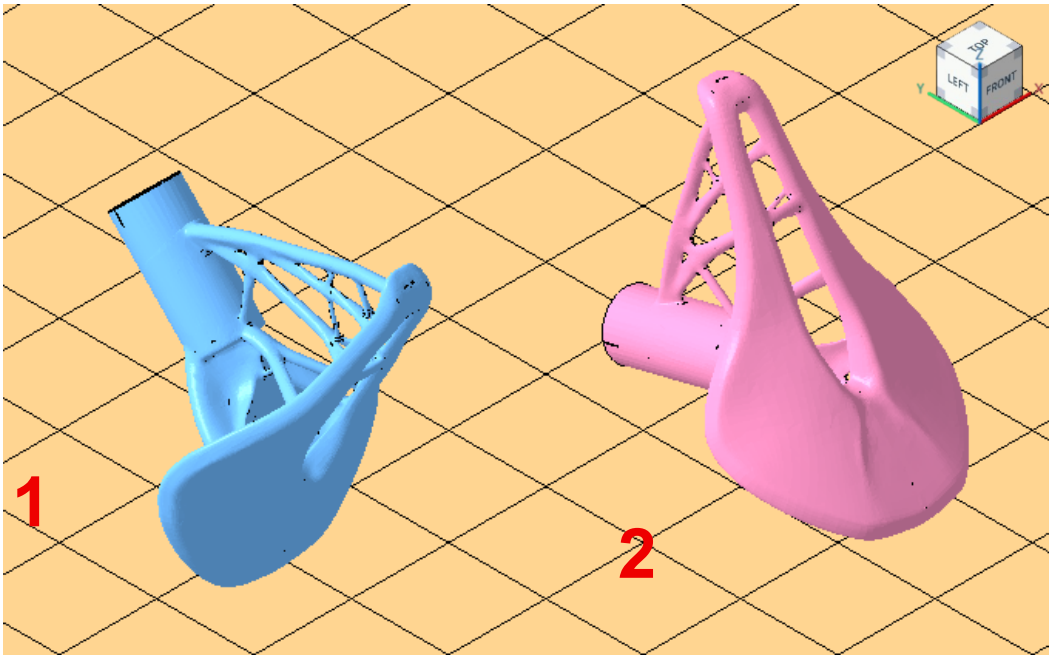

Figure 3.21: Part 6**:** Best orientation with RWTH method: 1 Correlation, 2 Transferability

The results obtained from the correlation analysis and the Netfabb method are similar, both representing the most favourable configurations in terms of support structure optimization and reduction of the bounding box volume.

However, the correlation-based solution requires a greater amount of support material compared to the Netfabb solution. This discrepancy may be attributed to the resolution limitations of the RWTH method.

In the case of the transferability analysis, the results indicate a reduced presence of support structures in the branch areas, where the removal of the supports is critical due to the low thickness of the geometry. Nevertheless, the internal channel requires support, which introduces the drawback of difficult support removal. The comparison is reported in Figure 3.22.

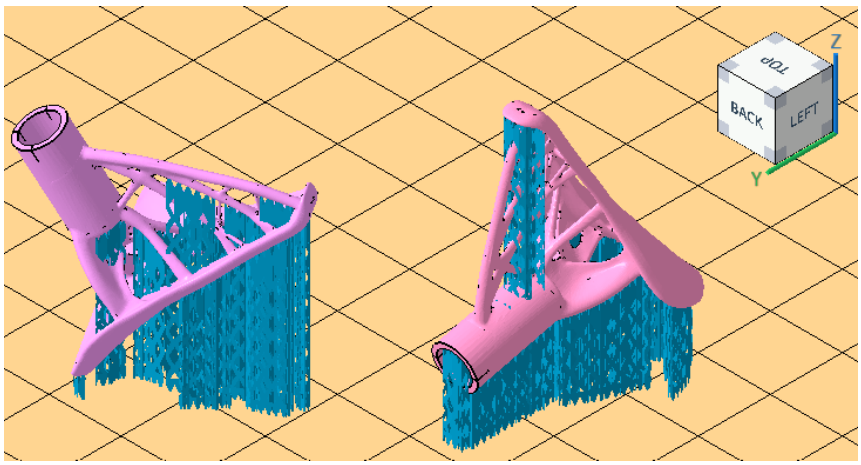

Figure 3.22: comparison of the support structures for the part 6

In this context, the Netfabb approach offers the most advantageous solution for minimizing geometric variation between successive layers and limiting large scanned areas, although the overall impact is less significant due to the slender geometry of the component. However, the RWTH method minimizes the risk of damage during the support removal stage, which represents a critical and complex stage in this technology.

The results are summarized in the Table 3.7:

Table 3.7: Part 6: comparative overview of advantages and disadvantages of the methods

Netfabb		**RWTH**	
Advantages	**Disadvantages**	**Advantages**	**Disadvantages**
Thermal management	Height	Less supports on the branches area	Height
Lower center of gravity	Supports on the branches area		Thermal management
			Supports in inner channels

3.7 Part 7

The optimal part orientation, as determined through the orientation optimization module in Netfabb, is illustrated in Figure 3.23.

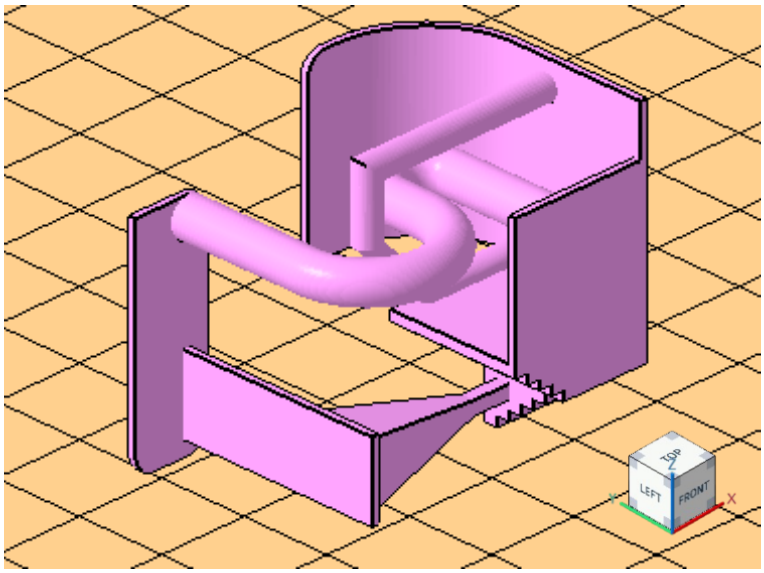

Figure 3.23: Part 7: best overall orientation with Netfabb

The best orientation for each of the parameter are reported in the Figure 3.24

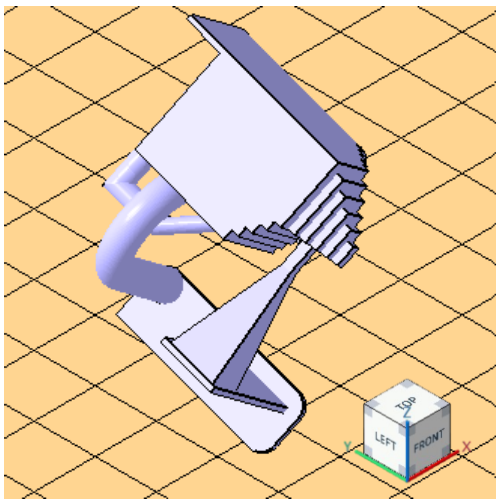

a. Supported area

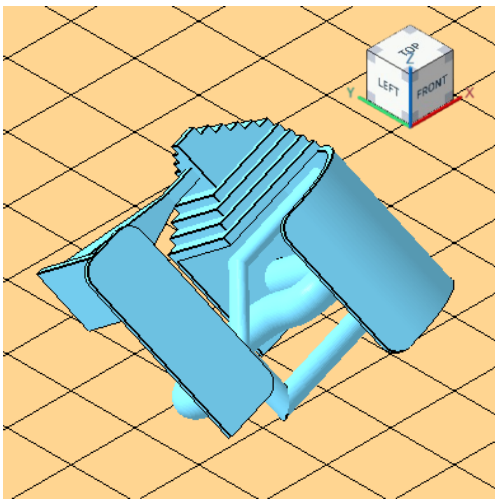

b. Supported volume

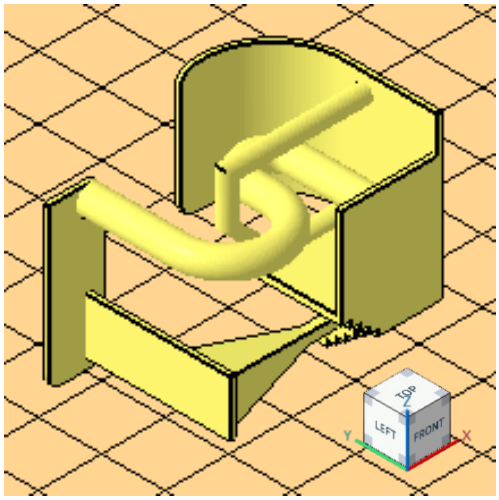

c. Bounding box volume

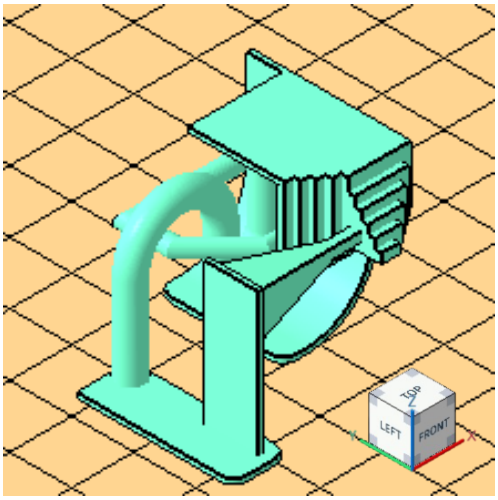

d. Height

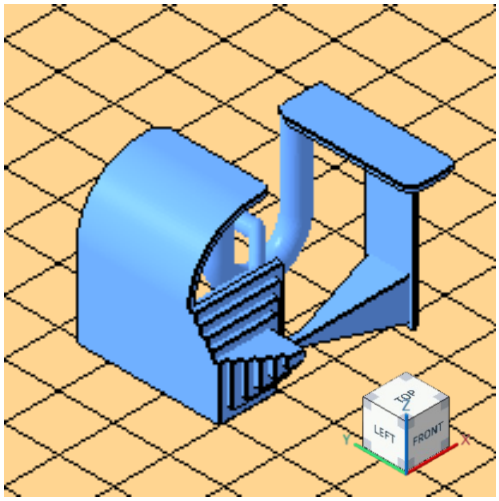

e. Center of gravity

Figure 3.24: Part 7: best orientation for each parameter with Netfabb

The outcomes of the orientation optimization method developed at RWTH Aachen University are presented, including both the correlation and transferability analyses. The results of these two studies are illustrated in Figure 3.25.

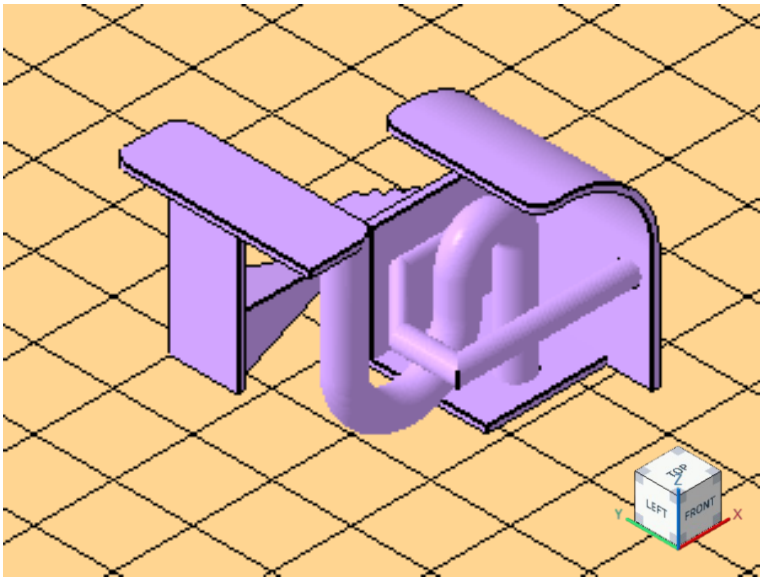

Figure 3.25: Part 7: Best orientation with RWTH method: correlation and transferability coincide

The orientation proposed by Netfabb corresponds to the one that optimizes the bounding box volume, while also achieving a favourable trade-off among the remaining parameters, particularly height and center of gravity. The presence of support structures is significant, as they are built directly onto the part, increasing the time required for their removal.

The RWTH method yields a similar solution, characterized by the presence of thin vertical or horizontal walls. This feature represents a critical aspect, as it may lead to issues during the printing process, such as part collapse due to collisions with the recoater. However, both orientations result in a relatively low number of layers.

Overall, the two approaches produce comparable results, with a reduction in build time. This benefit, however, comes at the expense of suboptimal support management and the inclusion of structures prone to failure.

.

The results are summarized in the Table 3.8:

Table 3.8: Part 7: comparative overview of advantages and disadvantages of the methods

Netfabb		**RWTH**	
Advantages	**Disadvantages**	**Advantages**	**Disadvantages**
Height	Vertical thin wall	Height	Vertical thin wall
	Supports		Supports

3.8 Part 8

Figure 3.26 represents the best overall orientation identified through Netfabb's orientation optimization process.

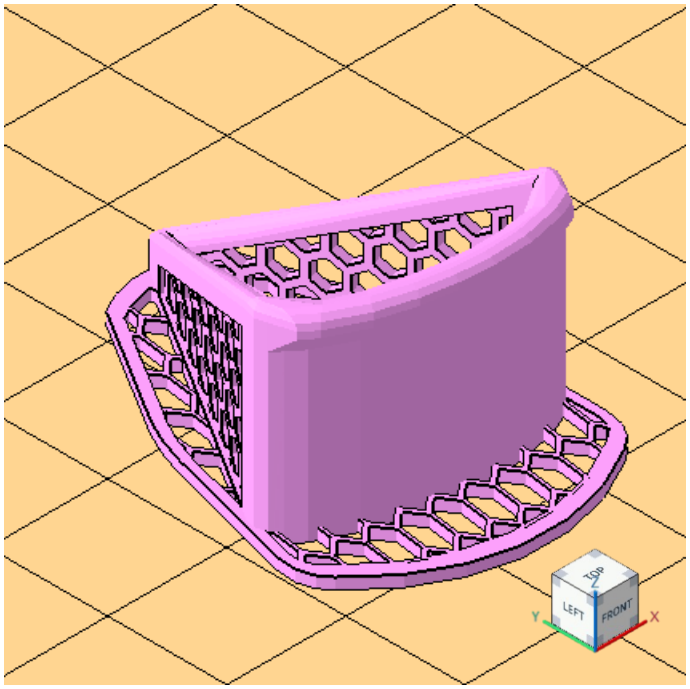

Figure 3.26: Part 8: best overall orientation with Netfabb

The optimal orientation for each parameter is shown in Figure 3.27.

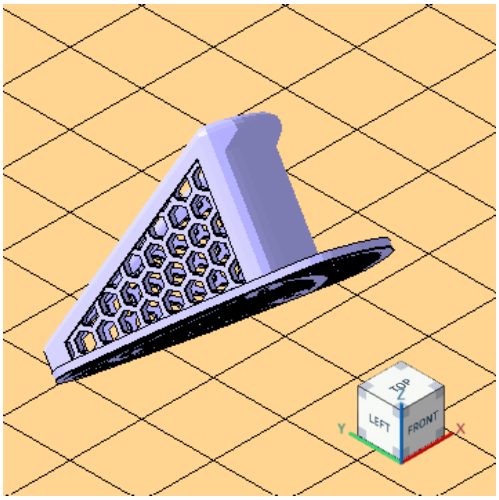

a. Supported area

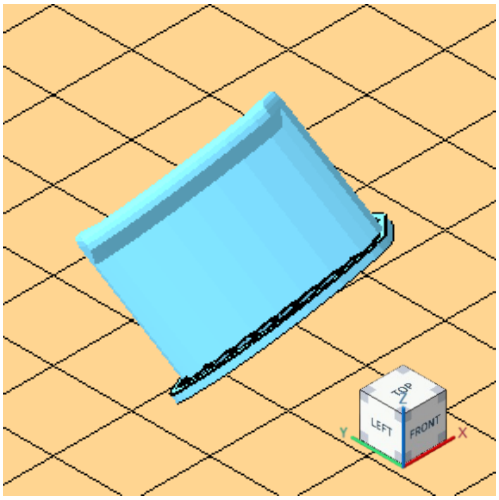

b. Supported volume

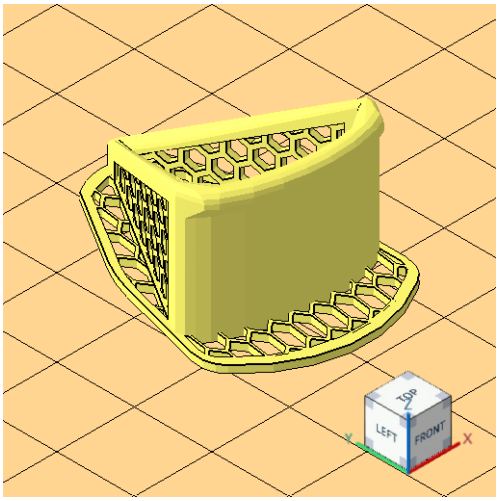

c. Bounding box volume

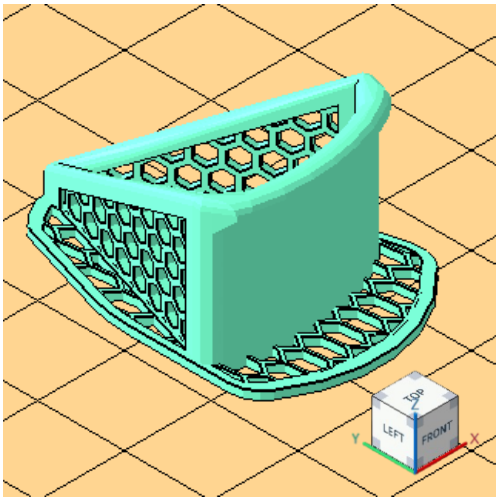

d. Height

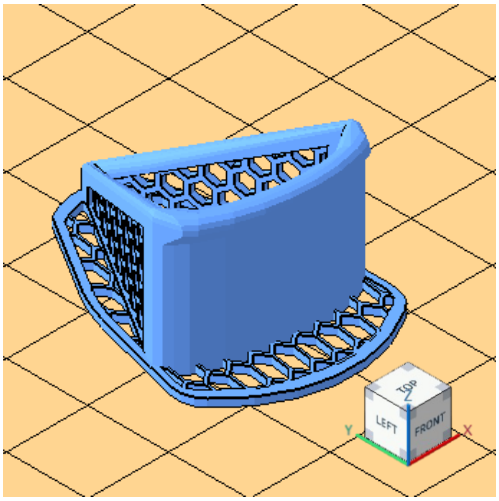

e. Center of gravity

Figure 3.27: Part 8: best orientation for each parameter with Netfabb

The results of the orientation optimization approach proposed by RWTH Aachen University are reported, with a focus on both the correlation analysis and the transferability study. These findings are visualized in Figure 3.28.

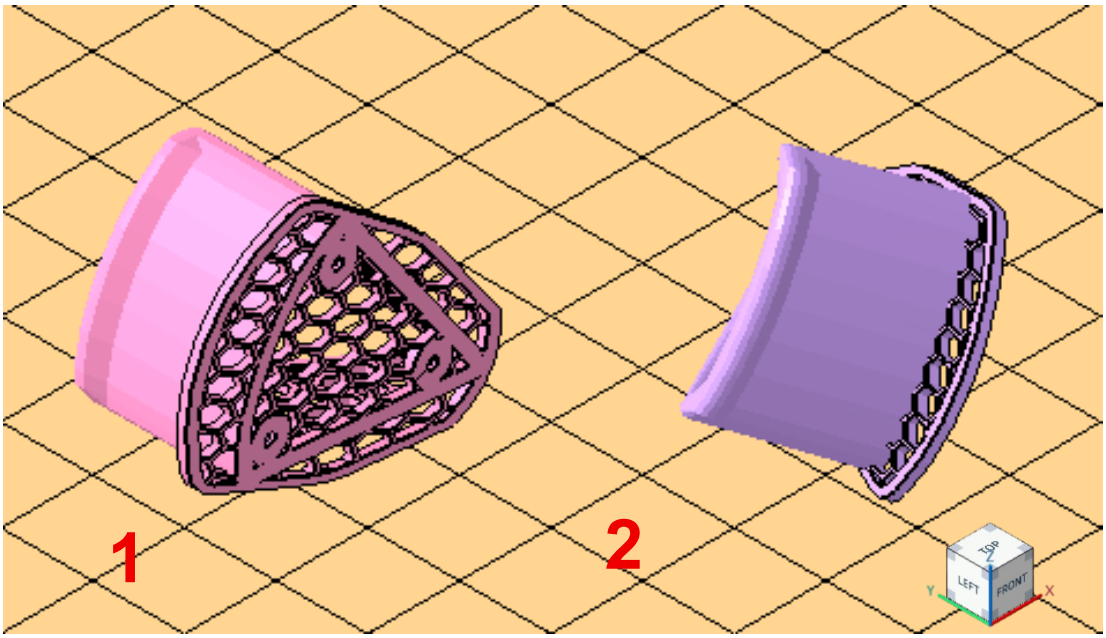

Figure 3.28: Part 8: Best orientation with RWTH method: 1 Correlation, 2 Transferability

The orientation for this part determined by Netfabb is driven by bounding box volume, Height, center of gravity. The support structures are present in vertical grid this can cause difficulties in the removing process. Additionally, there is an abrupt change of scanned surface between horizontal and vertical grid.

In contrast the solution offered by the RWTH method involves fewer support structures directly attached to the part, although the overall amount of support material is greater than in the Netfabb solution. The details of the supports are reported in the Figure 3.29:

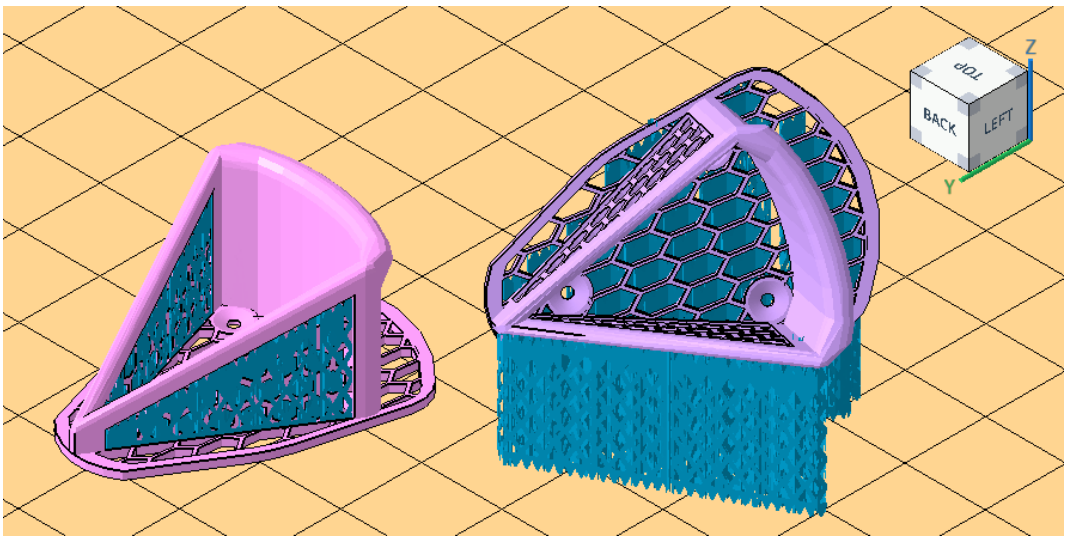

Figure 3.29: comparison of the support structures

Netfabb favours contact with the build plate and a reduced part height, which enhance printing speed and improve stability. Conversely, RWTH approach provides superior thermal management and support generation, which are fundamental parameters in PBF-LB/M processes.

The results are summarized in the Table 3.9.

Table 3.9: Part 8: comparative overview of advantages and disadvantages of the methods

Netfabb		**RWTH**	
Advantages	**Disadvantages**	**Advantages**	**Disadvantages**
Height	Thermal management	Thermal management	Height
Center of gravity			Center of gravity
Supports			Supports

4 Conclusion

This thesis has addressed the optimization of build orientation in Additive Manufacturing, with a specific focus on PBF-LB/M processes. The study critically compared two methodologies: the commercial multi-objective optimization tool Autodesk Netfabb and a novel algorithm developed at RWTH Aachen University, which utilizes six geometry-derived KPIs to assess deformation risk.

The analysis demonstrated that the RWTH method achieves, on average, a moderate correlation between the computed overall KPI and the observed deformations, thereby highlighting the potential of this type of solution. However, Tests performed on data transferability show a low correlation with deformations. A single KPI was identified as the primary driver of the deformation prediction, significantly affecting the overall results. In conclusion, it can be stated that currently ranking orientations, based only on KPIs deriving from geometry, is not yet feasible with adequate accuracy, despite promising correlations found between deformations and geometric KPIs.

Netfabb presents a neutral approach that is well suited for industrial applications, focusing on the minimization of support structures, build height, and bounding volume. The primary distinction between the two methods lies in their underlying strategies: while Netfabb employs a general-purpose approach, the RWTH algorithm adopts an approach specific to a single technology. More precisely, the RWTH method has been developed explicitly for PBF-LB/M and is grounded in thermal considerations related to part geometry in order to minimize deformation.

A comparison of the orientations generated by the two methods reveals substantial differences in the majority of cases. Netfabb, as a general approach, optimizes global parameters such as total height and center of gravity position. Conversely, the RWTH method provides more effective solutions from the perspective of thermal process management, with consequent advantages on residual stress and thermal deformation. The presence of support structures and the subsequent challenges in their removal do not indicate a clear advantage in support management for either method. In fact, the results vary across the different parts analysed.

Overall, the outcomes of the two methods align with their distinct optimization objectives. The developed algorithm demonstrates particular strengths through its incorporation of thermal history, which is critical for PBF-LB/M processes, whereas Netfabb provides more general advantages based on wider optimization criteria.

Finally, component orientation in AM remains a highly complex challenge due to the multitude of variables involved, including the diversity of technologies, the use of polymers or metals, and the variability within material types themselves. Moreover, determining an optimal solution often involves navigating trade-offs between competing factors. In this situation, the expertise of operators and designers becomes indispensable, as their ability to manage the inherent complexity and account for factors that are difficult to capture algorithmically is critical to achieving the most effective compromise. In this context, the developed model serves as a valuable support tool, offering a means to discriminate among a pre-selected set of orientations and facilitating the selection the optimal configuration, based on the thermal deformation predictions for the final component.

To ensure adequate applicability and reliability, the model requires further refinement and enhancement. This process should include the analysis of a broader range of geometries and orientations to strengthen predictive accuracy, as well as a more detailed investigation into the influence of specific features. Moreover, to generalize the findings and enhance their relevance for industrial applications it is essential to evaluate the effects of geometry and material properties, which were not considered in the present study. Lastly, conducting experiments on physical parts will serve as a valuable validation step. Testing under practical conditions will bridge the gap between predictions from thermal simulation and real-world conditions.

5 Bibliography

Adam, Guido A.O.; Zimmer, Detmar (2014): Design for Additive Manufacturing—Element transitions and aggregated structures. In: *CIRP Journal of Manufacturing Science and Technology* n. 1, 7, pp. 20–28. DOI: 10.1016/j.cirpj.2013.10.001.

Alkahari, Mohd Rizal; Furumoto, Tatsuaki; Ueda, Takashi; Hosokawa, Akira; Tanaka, Ryutaro; Aziz, Mohd (2012): Thermal Conductivity of Metal Powder and Consolidated Material Fabricated via Selective Laser Melting. In: *Key Engineering Materials,* 523-524, pp. 244–249. DOI: 10.4028/www.scientific.net/KEM.523-524.244.

Asapu, Sreekanth; Ravi Kumar, Y. (2025a): Design for Additive Manufacturing (DfAM): A Comprehensive Review with Case Study Insights. In: *JOM* n. 5, 77, pp. 3931–3951. DOI: 10.1007/s11837-025-07164-x.

Asapu, Sreekanth; Ravi Kumar, Y. (2025b): Design for Additive Manufacturing (DfAM): A Comprehensive Review with Case Study Insights. In: *JOM* n. 5, 77, pp. 3931–3951. DOI: 10.1007/s11837-025-07164-x.

B. K, Nagesha; K, Vinodh; Tigga, Amit Kumar; Barad, Sanjay; S, Anand Kumar (2021): Influence of post-processing techniques on residual stresses of SLM processed HPNGV. In: *Journal of Manufacturing Processes,* 66, pp. 189–197. DOI: 10.1016/j.jmapro.2021.04.020.

Bacciaglia, Antonio; Liverani, Alfredo; Ceruti, Alessandro (2024): Efficient part orientation algorithm for additive manufacturing in industrial applications. In: *The International Journal of Advanced Manufacturing Technology* n. 11, 133, pp. 5443–5462. DOI: 10.1007/s00170-024-14039-z.

Buchbinder, Damien; Meiners, Wilhelm; Pirch, Norbert; Wissenbach, Konrad; Schrage, Johannes (2013): Investigation on reducing distortion by preheating during manufacture of aluminum components

using selective laser melting. In: *J. Laser Appl.* n. 1, 26, p. 12004. DOI: 10.2351/1.4828755.

Calignano, Flaviana; Giuffrida, Federico; Galati, Manuela (2021): Effect of the build orientation on the mechanical performance of polymeric parts produced by multi jet fusion and selective laser sintering. In: *Journal of Manufacturing Processes,* 65, pp. 271–282. DOI: 10.1016/j.jmapro.2021.03.018.

Chand, Ramesh; Sharma, Vishal S.; Trehan, Rajeev; Gupta, Munish Kumar; Sarikaya, Murat (2023): Investigating the Dimensional Accuracy and Surface Roughness for 3D Printed Parts Using a Multi-jet Printer. In: *Journal of Materials Engineering and Performance* n. 3, 32, pp. 1145–1159. DOI: 10.1007/s11665-022-07153-0.

deep-geometry. https://deep-geometry.github.io/abc-dataset/.

Di Wang; Yang, Yongqiang; Yi, Ziheng; Su, Xubin (2013): Research on the fabricating quality optimization of the overhanging surface in SLM process. In: *The International Journal of Advanced Manufacturing Technology* n. 9, 65, pp. 1471–1484. DOI: 10.1007/s00170-012-4271-4.

Djokikj, Jelena; Kandikjan, Tatjana (2023): DfAM: Application of the design rules in the early design stages. In: *Procedia CIRP,* 118, pp. 659–663. DOI: 10.1016/j.procir.2023.06.113.

González, A.; Barea, R.; Corbera, S. (2025): A new temperature index for build orientation optimization in powder bed fusion additive manufacturing. In: *Additive Manufacturing,* 99, p. 104660. DOI: 10.1016/j.addma.2025.104660.

Leutenecker-Twelsiek, Bastian; Klahn, Christoph; Meboldt, Mirko (2016): Considering Part Orientation in Design for Additive Manufacturing. In: *Procedia CIRP,* 50, pp. 408–413. DOI: 10.1016/j.procir.2016.05.016.

Li, Yifan; Teng, Zhenjie (2024): Effect of printing orientation on mechanical properties of SLA 3D-printed photopolymer. In: *Fatigue Fract Eng Mater Struct* n. 5, 47, pp. 1531–1545. DOI: 10.1111/ffe.14265.

Manikandan, P.; Venkatesan, K. (2024): The influence of linear energy density on density, defect formation, residual stress, microstructure, and texture in 310 austenitic stainless steel by laser powder bed fusion. In: *Journal of Manufacturing Processes,* 131, pp. 2191–2207. DOI: 10.1016/j.jmapro.2024.10.022.

Matos, Marina A.; Rocha, Ana Maria A. C.; Pereira, Ana I. (2020): Improving additive manufacturing performance by build orientation optimization. In: *The International Journal of Advanced Manufacturing Technology* n. 5, 107, pp. 1993–2005. DOI: 10.1007/s00170-020-04942-6.

Mayer, Thomas; Brändle, Gabriel; Schönenberger, Andreas; Eberlein, Robert (2020): Simulation and validation of residual deformations in additive manufacturing of metal parts. In: *Heliyon* n. 5, 6, e03987. DOI: 10.1016/j.heliyon.2020.e03987.

Mele, Mattia; Bergmann, André; Campana, Giampaolo; Pilz, Tony (2021): Experimental investigation into the effect of supports and overhangs on accuracy and roughness in laser powder bed fusion. In: *Optics & Laser Technology,* 140, p. 107024. DOI: 10.1016/j.optlastec.2021.107024.

Mele, Mattia; Campana, Giampaolo; Bergmann, André (2022): Optimisation of part orientation and design of support structures in laser powder bed fusion. In: *Int J Interact Des Manuf* n. 2, 16, pp. 597–611. DOI: 10.1007/s12008-022-00856-7.

Mercelis, Peter; Kruth, Jean-Pierre (2006): Residual stresses in selective laser sintering and selective laser melting. In: *Rapid Prototyping Journal* n. 5, 12, pp. 254–265. DOI: 10.1108/13552540610707013.

Mertens, Anne; Delahaye, Jocelyn; Dedry, Olivier; Vertruyen, Bénédicte; Tchuindjang, Jérôme T.; Habraken, Anne Marie (2020): Microstructure and Properties of SLM AlSi10Mg: Understanding the Influence of the Local Thermal History. In: *Procedia Manufacturing,* 47, pp. 1089–1095. DOI: 10.1016/j.promfg.2020.04.121.

Oliveira, J. P.; LaLonde, A. D.; Ma, J. (2020): Processing parameters in laser powder bed fusion metal additive manufacturing. In: *Materials & Design,* 193, p. 108762. DOI: 10.1016/j.matdes.2020.108762.

Palmeri, D.; Buffa, G.; Pollara, G.; Fratini, L. (2022): Sample building orientation effect on porosity and mechanical properties in Selective Laser Melting of Ti6Al4V titanium alloy. In: *Materials Science and Engineering: A,* 830, p. 142306. DOI: 10.1016/j.msea.2021.142306.

Parry, L. A.; Ashcroft, I. A.; Wildman, R. D. (2019): Geometrical effects on residual stress in selective laser melting. In: *Additive Manufacturing,* 25, pp. 166–175. DOI: 10.1016/j.addma.2018.09.026.

printables. https://www.printables.com/.

Qin, Yuchu; Qi, Qunfen; Scott, Paul J.; Jiang, Xiangqian (2019): Determination of optimal build orientation for additive manufacturing using Muirhead mean and prioritised average operators. In: *Journal of Intelligent Manufacturing* n. 8, 30, pp. 3015–3034. DOI: 10.1007/s10845-019-01497-6.

Ranjan, Rajit; Ayas, Can; Langelaar, Matthijs; van Keulen, Fred (2020): Fast Detection of Heat Accumulation in Powder Bed Fusion Using Computationally Efficient Thermal Models. In: *Materials* n. 20, 13. DOI: 10.3390/ma13204576.

Ransikarbum, Kasin; Pitakaso, Rapeepan; Kim, Namhun; Ma, Jungmok (2021): Multicriteria decision analysis framework for part orientation analysis in additive manufacturing. In: *J Comput Des Eng* n. 4, 8, pp. 1141–1157. DOI: 10.1093/jcde/qwab037.

Raut, Sandeep; Jatti, VijayKumar S.; Khedkar, Nitin K.; Singh, T. P. (2014): Investigation of the Effect of Built Orientation on Mechanical Properties and Total Cost of FDM Parts. In: *Procedia Materials Science,* 6, pp. 1625–1630. DOI: 10.1016/j.mspro.2014.07.146.

Sedighi, Iman; Ayatollahi, Majid R.; Bahrami, Bahador; Pérez-Martínez, Marco A.; Garcia-Granada, Andres A. (2020): Mechanical behavior of an additively manufactured poly-carbonate specimen: tensile,

flexural and mode I fracture properties. In: *Rapid Prototyping Journal* n. 2, 26, pp. 267–277. DOI: 10.1108/RPJ-03-2019-0055.

Song, Xu; Feih, Stefanie; Zhai, Wei; Sun, Chen-Nan; Li, Feng; Maiti, Raj et al. (2020): Advances in additive manufacturing process simulation: Residual stresses and distortion predictions in complex metallic components. In: *Materials & Design,* 193, p. 108779. DOI: 10.1016/j.matdes.2020.108779.

Strano, Giovanni; Hao, Liang; Everson, Richard M.; Evans, Kenneth E. (2013): Surface roughness analysis, modelling and prediction in selective laser melting. In: *Journal of Materials Processing Technology* n. 4, 213, pp. 589–597. DOI: 10.1016/j.jmatprotec.2012.11.011.

Tabaie, Seyedmohammad; Rézaï-Aria, Farhad; Jahazi, Mohammad (2020): Microstructure Evolution of Selective Laser Melted Inconel 718: Influence of High Heating Rates. In: *Metals* n. 5, 10. DOI: 10.3390/met10050587.

thingiverse. https://www.thingiverse.com/.

Tucho, Wakshum M.; Lysne, Vidar H.; Austbø, Håkon; Sjolyst-Kverneland, Atle; Hansen, Vidar (2018): Investigation of effects of process parameters on microstructure and hardness of SLM manufactured SS316L. In: *Journal of Alloys and Compounds,* 740, pp. 910–925. DOI: 10.1016/j.jallcom.2018.01.098.

Turek, Paweł; Bazan, Anna; Bulicz, Marcin (2024): Effect of 3D Printing Orientation on the Accuracy and Surface Roughness of Polycarbonate Samples. In: *Machines,* 13, p. 9. DOI: 10.3390/machines13010009.

Vafadar, Ana; Guzzomi, Ferdinando; Rassau, Alexander; Hayward, Kevin (2021): Advances in Metal Additive Manufacturing: A Review of Common Processes, Industrial Applications, and Current Challenges. In: *Applied Sciences* n. 3, 11. DOI: 10.3390/app11031213.

Willems, Jörg; Megahed, Mustafa (2022): A numerical formalism towards finding a good component orientation in laser powder bed fusion. In:

Additive Manufacturing Letters, 2, p. 100031. DOI: 10.1016/j.addlet.2022.100031.

Yi, J. H.; Kang, J. W.; Wang, T. J.; Wang, X.; Hu, Y. Y.; Feng, T. et al. (2019): Effect of laser energy density on the microstructure, mechanical properties, and deformation of Inconel 718 samples fabricated by selective laser melting. In: *Journal of Alloys and Compounds,* 786, pp. 481–488. DOI: 10.1016/j.jallcom.2019.01.377.

Zhang, Yicha; Bernard, Alain; Harik, Ramy; Karunakaran, K. P. (2017): Build orientation optimization for multi-part production in additive manufacturing. In: *Journal of Intelligent Manufacturing* n. 6, 28, pp. 1393–1407. DOI: 10.1007/s10845-015-1057-1.

Zwier, Marijn P.; Wits, Wessel W. (2016): Design for Additive Manufacturing: Automated Build Orientation Selection and Optimization. In: *Procedia CIRP,* 55, pp. 128–133. DOI: 10.1016/j.procir.2016.08.040.